Sedimentary resurfacing and fretted terrain development along the crustal dichotomy boundary, Aeolis Mensae, Mars

Rossman P. Irwin III[1] and Thomas R. Watters

Center for Earth and Planetary Studies, National Air and Space Museum, Smithsonian Institution, Washington, D. C., USA

Alan D. Howard

Department of Environmental Sciences, University of Virginia, Charlottesville, Virginia, USA

James R. Zimbelman

Center for Earth and Planetary Studies, National Air and Space Museum, Smithsonian Institution, Washington, D. C., USA

Received 6 February 2004; accepted 1 June 2004; published 30 September 2004.

[1] The evolution of the Martian crustal dichotomy boundary, which separates the southern cratered highlands from the northern lowland plains by 1–3 km of elevation, remains among the fundamental outstanding issues in Mars research. For a study area at Aeolis Mensae we show that fretted terrain formed exclusively in a >2 km thick, late Noachian (~3.7 Ga) sedimentary deposit that overlies the base of an older, cratered dichotomy boundary slope. In this equatorial study area, fretted terrain does not exhibit the debris aprons or lineated valley fills that are attributed to ground ice in otherwise similar, midlatitude fretted terrain in Arabia Terra. The massive deposit of fine sand or loess was probably transported from the north by wind and trapped against the precursor dichotomy slope, producing a similar initial form to the younger Medusae Fossae layered materials that occur east of Aeolis Mensae. Contemporary with the latest Noachian to early Hesperian decline in fluvial erosion, the fretting process likely initiated as the massive layer's indurated surface was compromised by fracture, cratering, or collapse into possible voids. In these depressions, grain impact or contact with water disaggregated the fine sedimentary materials, which were then largely deflated by wind. The fretting process largely ended when liquid water was no longer widely available for weathering during the early Hesperian period, although some degradation of the region by aeolian and slope processes has continued to the present. *INDEX TERMS:* 5415 Planetology: Solid Surface Planets: Erosion and weathering; 5470 Planetology: Solid Surface Planets: Surface materials and properties; 6207 Planetology: Solar System Objects: Comparative planetology; 6225 Planetology: Solar System Objects: Mars; *KEYWORDS:* Aeolis Mensae, fretted terrain, sedimentary deposits

Citation: Irwin, R. P., III, T. R. Watters, A. D. Howard, and J. R. Zimbelman (2004), Sedimentary resurfacing and fretted terrain development along the crustal dichotomy boundary, Aeolis Mensae, Mars, *J. Geophys. Res.*, *109*, E09011, doi:10.1029/2004JE002248.

1. Introduction

[2] The Martian crustal dichotomy is a pronounced topographic break of 1–3 km in elevation, separating ancient cratered highlands located predominantly in the Southern Hemisphere from smooth, younger lowland plains to the north (e.g., Aeolis Mensae study area in Figure 1a). The origin of the dichotomy remains among the major outstanding questions in Mars research. Theories for its origin include endogenic and exogenic mechanisms, with the former category generally invoking degree 1 convective overturn of the mantle and crustal thinning to form the lowlands [*Lingenfelter and Schubert*, 1973; *Wise et al.*, 1979; *Davies and Arvidson*, 1981; *Janle*, 1983; *McGill and Dimitriou*, 1990; *Zhong and Zuber*, 2001]. *Sleep* [1994] proposed a plate tectonic scenario to explain the dichotomy. Exogenic mechanisms involve one giant impact [*Wilhelms and Squyres*, 1984] or multiple [*Frey and Schultz*, 1988, 1990] giant impacts into the Northern Hemisphere, resulting in a net redistribution of material into the southern highlands. *McGill and Squyres* [1991] and *Zuber* [2001] reviewed theories for the origin of the crustal dichotomy. More recently, *Watters* [2003a, 2003b] suggested that the dichotomy boundary (a transitional zone between cratered

[1]Also at Department of Environmental Sciences, University of Virginia, Charlottesville, Virginia, USA.

0148-0227/04/2004JE002248$09.00

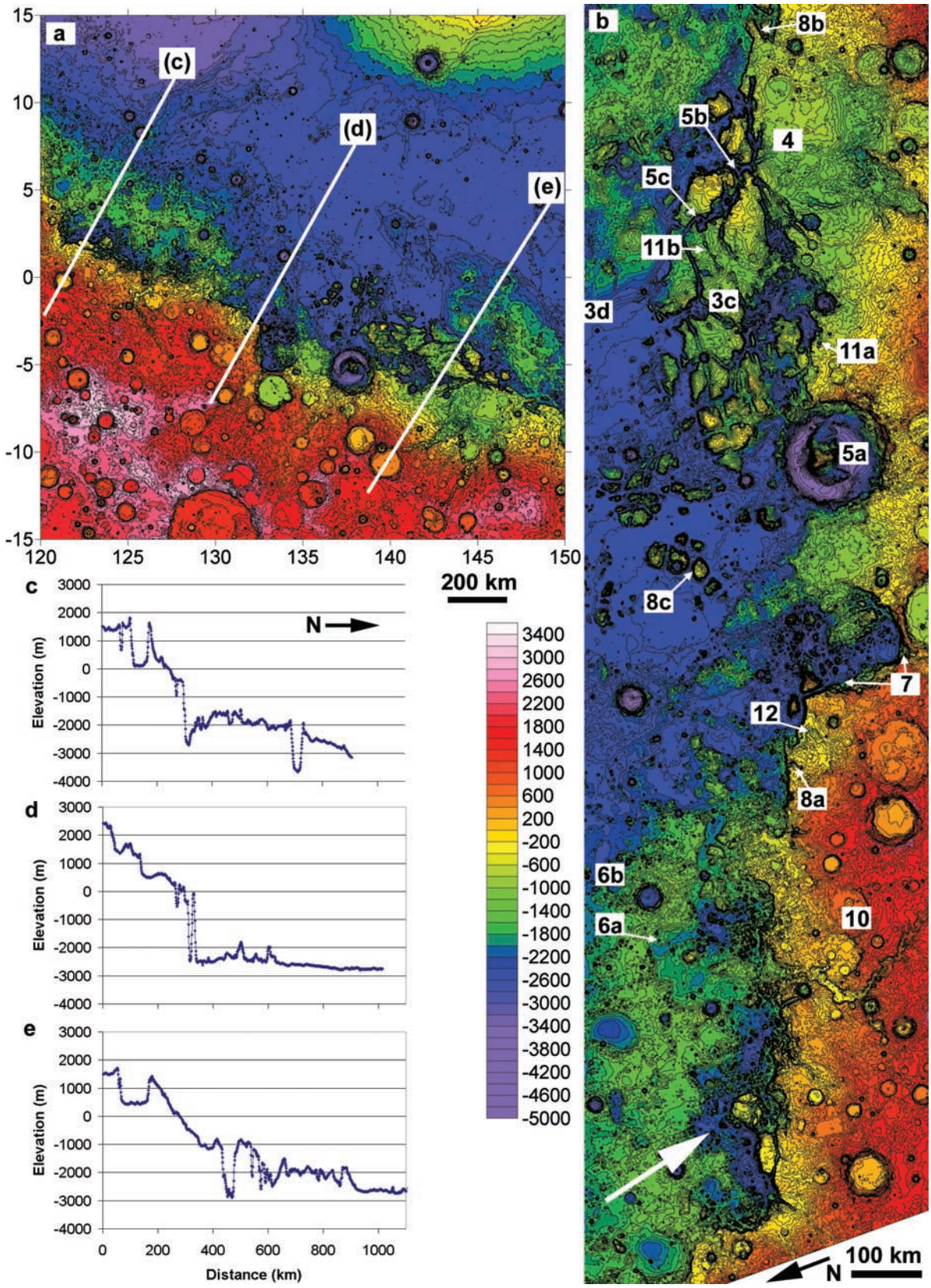
a
(c)
(d)
(e)
15
10
5
0
-5
-10
-15
120
125
130
135
140
145
150
200 km
b
8b
5b
4
5c
11b
3d
3c
11a
5a
8c
7
12
8a
6b
6a
10
100 km
N
c
d
e
Elevation (m)
3000
2000
1000
0
-1000
-2000
-3000
-4000
N
0
200
400
600
800
1000
Distance (km)
3400
3000
2600
2200
1800
1400
1000
600
200
-200
-600
-1000
-1400
-1800
-2200
-2600
-3000
-3400
-3800
-4200
-4600
-5000

Figure 1

highlands and lowland plains, rather than a linear feature) underwent flexure induced by loading of the northern lowlands. Counts of buried lowland impact craters constrain the age of the lowland crust (and perhaps the dichotomy itself) to the early Noachian period [*Frey et al.*, 2002], to which *Hartmann and Neukum* [2001] apply an age of >3.95 Ga.

[3] Significant erosion and burial of the dichotomy boundary occurred from its time of formation into the early Hesperian period [*Neukum and Hiller*, 1981; *Maxwell and McGill*, 1988; *McGill*, 2000] (until 3.6 Ga [*Hartmann and Neukum*, 2001]). These modifications are contemporary with or postdate the declining cratering rates [*Hartmann and Neukum*, 2001], waning fluvial activity [*Craddock and Maxwell*, 1990], and reverse faulting along the dichotomy boundary [*Watters and Robinson*, 1999]. Erosion of the boundary included late Noachian to early Hesperian development of knobby and fretted terrains from high-standing surfaces (Figures 2 and 3a–3c). Lacking an established terrestrial analogue, the fretting process has remained poorly understood to the present [*Carr*, 2001]. In fretted areas, broad, flat-floored valleys isolate large mesas and knobs with up to 2 km of relief (Figures 1–3), or the fretted valleys occur as deep reentrants into high-standing terrain with limited tributary development (Figure 2) [*Sharp*, 1973]. Most studies of the dichotomy boundary morphology have focused on the midlatitude fretted terrain on the northern margin of Arabia Terra. In this region, late Noachian and early Hesperian structural [*McGill and Dimitriou*, 1990] and/or fluvial processes [*Carr*, 2001] may have initially isolated the mesas, as indicated by an irregular grid pattern or linear trend to most valleys, along with some sinuous valleys that deeply dissect the adjacent highlands (Figure 2b). Ice-facilitated mass wasting is interpreted to be responsible for Amazonian degradation of this region [*Squyres*, 1978; *Lucchitta*, 1984; *Mangold and Allemand*, 2001; *Mangold*, 2003], forming the characteristic lineated valley fill and debris aprons around mesas and valley walls (Figures 3a and 3b) after the fretted valleys were incised [*Squyres*, 1978].

[4] Knobby terrain consists of smaller isolated hills with flat or rounded summits, which are often located north (downslope) of the fretted terrains along the dichotomy boundary. The knobs decrease in size and density with distance from the boundary (Figure 2b), suggesting that this knobby terrain represents a late stage in the degradation of fretted terrain mesas [*Sharp*, 1973]. Volcanic flows have buried the dichotomy boundary in the Tharsis region [*Scott and Tanaka*, 1986]. From Tharsis west to Aeolis Mensae, sedimentary materials of the Medusae Fossae Formation bury parts of the dichotomy boundary (Figure 3d) [*Scott and Tanaka*, 1986; *Greeley and Guest*, 1987]. Medusae Fossae is thought to be a relatively young, friable, aeolian sedimentary deposit of sand or volcanic ash [*Bradley et al.*, 2002; *Hynek et al.*, 2003].

[5] This paper focuses on the history of modifications to one section of the dichotomy boundary, including the development of fretted and knobby terrains in Aeolis Mensae (10°N–10°S, 120°–150°E, Figure 1). By evaluating the geomorphic processes that have affected the dichotomy boundary throughout its history, we isolate ancient features of the dichotomy and distinguish these from younger landforms that developed under different circumstances. The purpose of this paper is not to settle the issue of the dichotomy's origin, which would require a detailed examination of large-scale, ancient endogenic and exogenic mechanisms during a time that is poorly represented by the geologic record. We discuss evidence for several distinct geologic material units in the region, noting that fretted terrain is confined to a likely sedimentary deposit with distinct morphologic and thermal properties. We then discuss geomorphic processes that have affected these terrain units relative to the time-stratigraphic scale of *Tanaka* [1986]. This analysis relies on a critical rationalist approach [*Bartley*, 1964], whereby Earth-based process-form relationships are used to evaluate alternate hypotheses for the origin of Martian landforms.

2. Features of the Study Area

[6] Broadly similar fretted terrains occur along the dichotomy boundary in Arabia Terra (~25°–50°N, 10°–80°E) and at the present study area, Aeolis Mensae (10°N–10°S, 120°–150°E) (Figure 2), but the two regions exhibit some morphologic dissimilarities (Figure 3). Isolated mesas and knobs occur in both areas, transitioning to smaller knobs with rounded summits at greater distances from the dichotomy scarp. Both areas also contain elongated reentrants into high-standing surfaces, which originate at chains of closed depressions or are connected to sinuous, branching (likely fluvial) highland valleys. However, fretted terrains in the equatorial region do not exhibit lineated valley fill and debris aprons, which are distinctive in the higher latitudes (>30°) north of Arabia Terra (Figures 3a and 3b). The low crater density on debris aprons [*Mangold*, 2000, 2003], the irregular floor topography of sinuous fretted valleys due to apron development [*Lanz et al.*, 2000; *Carr*, 2001], and the likely development of lineated fill from cross-valley (rather than down-valley) mass wasting [*Carr*, 2001] support development of debris aprons after the primary terrain fretting process had ceased [*Squyres*, 1978]. The Aeolis Mensae region valleys are also more sharply defined, with less rounding of valley wall crests

Figure 1. Topography of the study area from the 128 pixel/degree Mars Observer Laser Altimeter (MOLA) topographic grid. (a) Study area showing tracks of topographic profiles in areas c, d, and e. (b) Enlargement of fretted and knobby terrains along the boundary, showing locations of images in other figures. Note change in orientation relative to Figure 1a. Gale Crater is the location of area 5a. The western side of the study area is dominated by several closed depressions (large white arrow) that formed in an initial northward slope; smooth plains embay the center of the study area, and the eastern side contains the fretted plateau. The elevated ridge to the northeast of the fretted plateau is the Medusae Fossae Formation. (c) Cross section of the irregular closed depression in the knobby terrain. (d) Cross section of the most deeply eroded part of the boundary in the study area, where smooth plains embay remnant knobs of the fretted plateau. (e) Cross section of the fretted plateau at −1000 m, with an eroded ridge of Medusae Fossae Formation at −2000 m.

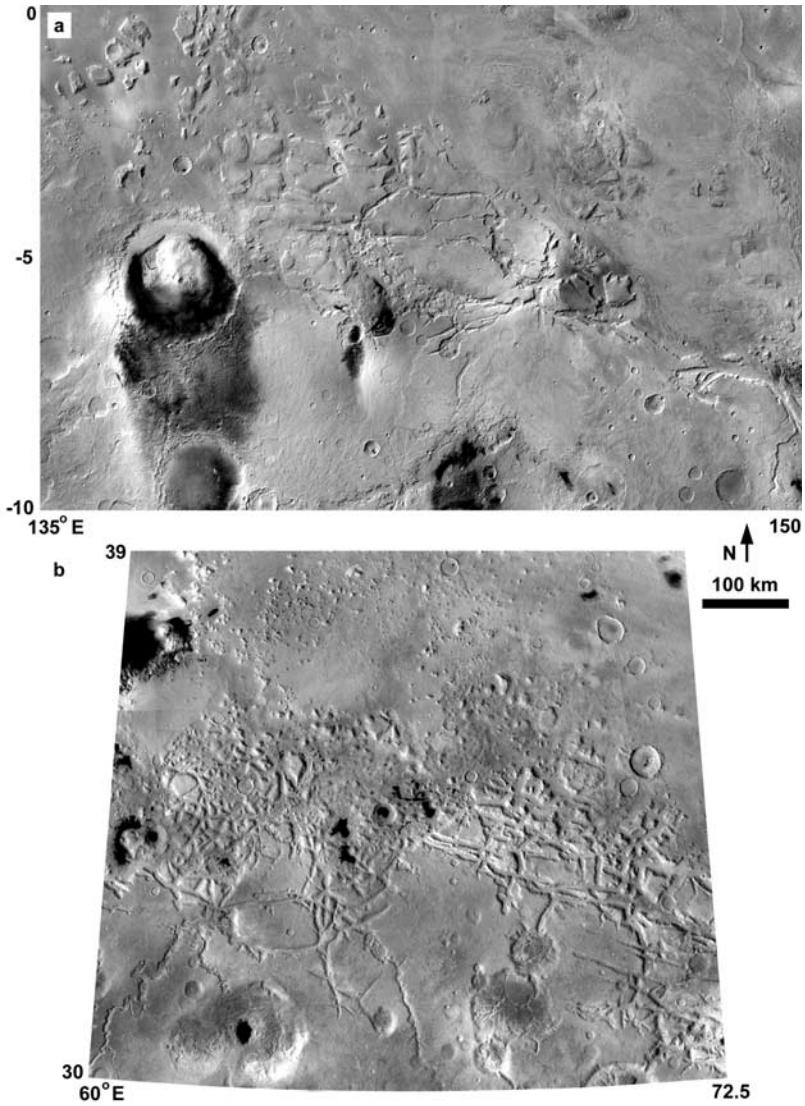

Figure 2. Comparison of fretted terrains in (a) Aeolis Mensae, 0°–10°S and 135°–150°E (within our study area), and (b) Nilosyrtis Mensae, 30°–39°N and 60°–72.5°E (outside of our study area), from the Mars Orbiter Camera (MOC) Geodesy Campaign Mosaic. In both cases, mesas are isolated from high-standing terrain and progressively degraded to knobs with distance northward into the lowlands. In Figure 2a the central mound of Gale Crater is the high-albedo feature to the center left.

(Figure 3c). Aeolis Mensae significantly demonstrates that some fretted terrain formed without developing or preserving debris aprons and lineated valley fill, so the formative processes of fretted terrain can be examined here without the younger ice-related landforms.

[7] In Aeolis Mensae, the dichotomy boundary terrain incorporates an initially low-gradient northward declivity (~0.4°, Figures 1c–1e), transitioning from cratered highland materials, through knobby and fretted terrains, and terminating in the smooth lowland plains. Valley networks are abundant in the highlands but are generally absent in the fretted terrain and lowlands. In the western portion of the study area an elongated, irregular enclosed basin containing mesas and knobs interrupts the boundary slope, which appears to continue on both sides of the basin (Figures 1b and 1c). The terrain in and around this closed basin has been identified as "knobby" [*King*, 1978; *Hiller*, 1979] or "undifferentiated" [*Greeley and Guest*, 1987] terrain in geologic maps. As these mapped boundaries define terrain units rather than geologic materials in many cases, we note when specific geologic materials are discussed.

[8] To the east of this enclosed basin the dichotomy boundary slope includes an abrupt scarp (commonly ~10°–30° slope) at its base, with outlying mesas to the north (Figure 1d). Amazonian smooth lowland plains embay these mesas in the central part of the study area (Figure 3d). These plains are nearly level in Mars Observer Laser Altimeter (MOLA) topography (Figure 1d) and are likely associated with the Elysium Mons volcano, although recent aqueous outflows have also modified the Elysium plains [*Tanaka*, 1986; *Greeley and Guest*, 1987; *Tanaka et al.*, 1992]. These smooth plains also embay a fretted plateau to the east, which previous mappers recognized as a

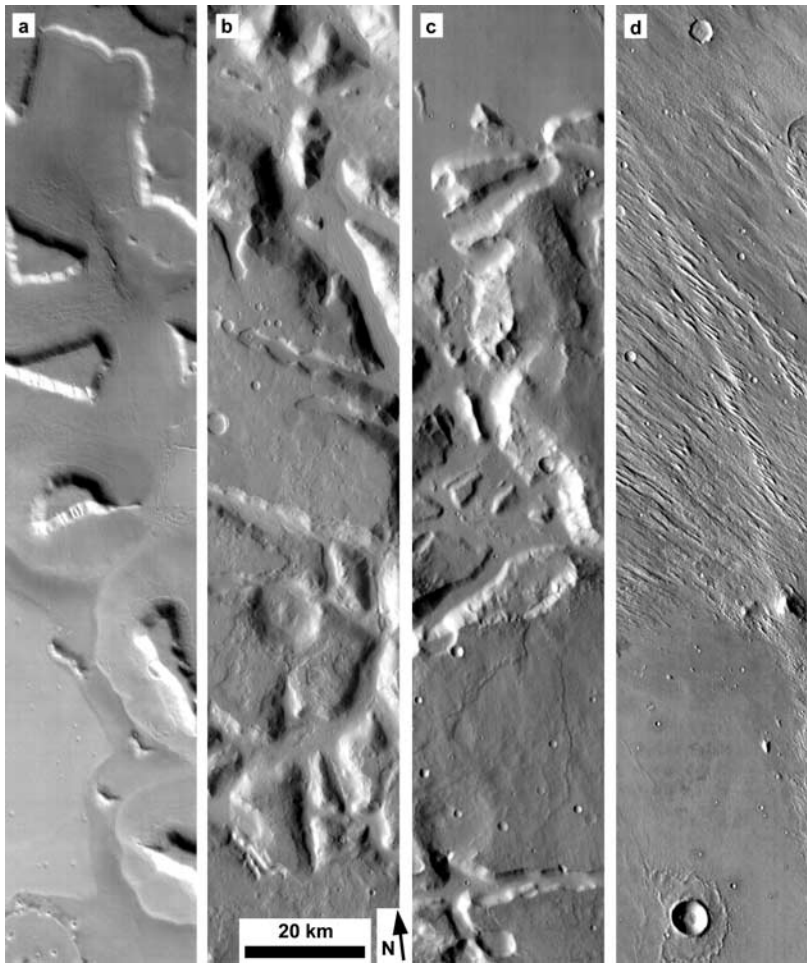

Figure 3. Contrast of (a and b) terrains north of Arabia Terra with (c and d) those in the study area. Figure 3a (Thermal Emission Imaging System (THEMIS) image I01185003) shows mesas with debris aprons in Deuteronilus Mensae, 44.5°N and 27.5°E. Figure 3b (THEMIS image I04454002) shows fretted valleys with lineated valley fill and subdued valley crests in Nilosyrtis Mensae, 31.8°N and 70.6°E. Figure 3c (THEMIS image I0730008) shows fretted valleys with no lineated valley fill or debris aprons and with sharp definition in Aeolis Mensae, 3.4°S and 142°E. Figure 3d (THEMIS image I0730008) shows Medusae Fossae yardangs and smooth plains surface, 0°N and 142.5°E.

geologic material unit distinct from and overlying the cratered plains. *Scott et al.* [1978] mapped this high-standing unit as ''plateau material,'' which formed smooth, high-standing, flat surfaces that had undergone dissection to form mesas and buttes. *Greeley and Guest* [1987] also differentiated the plateau materials from cratered terrain, lumping the plateau with other ''subdued cratered'' materials across Mars and suggesting an origin as a thin veneer of volcanic or sedimentary deposits over older rocks. The Medusae Fossae Formation overlies Elysium smooth plains and the fretted plateau to the northeast, making it the youngest material in the study area.

3. Aeolis Mensae Geologic Materials

3.1. Cratered Plains

[9] The oldest geologic materials in this study area are cratered plains materials (terrain units Npl_1 and Npld of *Greeley and Guest* [1987]). This material includes impact megabreccia at depth, overlaid by spatially variable proportions of impact ejecta, sedimentary deposits, and igneous materials. In this paper, cratered plains materials are defined as incorporating impact ejecta in some proportion; the term therefore distinguishes crater materials compositionally from finer-grained, well-sorted sediments that may locally mantle the surface of some mapped cratered plains terrain units [*Malin and Edgett*, 2000]. The highlands appear to be composed primarily of basalt and the products of mechanical and (perhaps to a lesser degree) chemical weathering of basalt [*Bandfield et al.*, 2000, 2003]. As the detailed stratigraphy and lithology for the cratered plains is not available, it is treated herein as a single material unit, with vertical heterogeneity on the order of 1 to $>10^2$ m. This heterogeneity is significant to the geomorphology of the unit. As many old (e.g., Hesperian) craters on Mars retain a pristine appearance, a fraction of the particle sizes in crater ejecta must be too coarse for aeolian transport, which is ineffective for grain diameters >2–4 mm [*Greeley and Iversen*, 1985]. Cratered plains materials can therefore be easily distinguished from superposed layered materials

that have been significantly deflated by wind [*Malin and Edgett*, 2000].

[10] Modification of cratered plains materials therefore requires either a relatively (to wind) robust sediment transport process, and/or antecedent weathering of coarse particles/bedrock to smaller grain sizes, which does not appear to have occurred en masse since the craters of Noachian/Hesperian boundary age were emplaced [*Craddock and Maxwell*, 1990]. To satisfy these requirements, Noachian aqueous erosion has been invoked as the most reasonable means for degrading contemporary impact craters, where the altered geometric profile and morphology of a crater suggest modification of the original crater materials rather than simple burial [*Craddock and Maxwell*, 1993; *Craddock et al.*, 1997]. The spatial and temporal coincidence of ancient valley networks with degraded highland impact craters supports this hypothesis. The ubiquitous valley networks and degraded craters in sloping areas of the adjacent highlands [*Irwin and Howard*, 2002] suggest that fluvial processes may have also affected the dichotomy boundary region, but the morphology of fretted and knobby terrains is substantially different from adjacent cratered plains. This disparity suggests that different processes or materials influenced the fretted terrain morphology, as we discuss through the rest of the paper.

3.2. Fretted Plateau and Knobby Terrains

[11] The most poorly understood terrain unit is the "plateau" [*Scott and Allingham*, 1976; *Scott et al.*, 1978; *King*, 1978; *Hiller*, 1979] or "subdued cratered" unit [*Greeley and Guest*, 1987], identified herein as "fretted plateau" within this study area. *Guest et al.* [1977] note that fretted terrain appears restricted to the mapped plateau materials in the Cydonia region (40–50°N, 15°W–10°E), north of Arabia Terra, and the relationship pertains to Aeolis Mensae as well. Erosion of this material to form-fretted terrain, with its broad valleys and undissected remnant mesas, involved spatially focused erosional processes unlike the ubiquitous processes that eroded impact craters throughout the adjacent Noachian highlands [*Strom et al.*, 1992; *Craddock and Maxwell*, 1993; *Irwin and Howard*, 2002]. Erosive processes in fretted terrain must also have been relatively efficient. Creating a fretted valley ~1 km deep in a time on the order of $\sim 10^8$ years implies an average erosion rate on the order of 10^{-2} mm yr^{-1}, assuming the *Hartmann and Neukum* [2001] chronology and development between the end of major highland crater degradation (Noachian/Hesperian boundary) and the end of the early Hesperian [*Neukum and Hiller*, 1981; *Maxwell and McGill*, 1988; *McGill*, 2000]. This rate is 1–2 orders of magnitude more rapid than the denudation rates indicated by degraded highland impact craters [*Craddock and Maxwell*, 1993]. The rapid rate and spatial constraint of the fretting processes invoke either relatively efficient, focused erosional processes in the fretted plateau or poorly resistant geologic materials compared to the cratered plains. This rapid erosion must have occurred without similarly affecting the adjacent highland cratered plains, where 20–100 m deep valley networks and other small, late Noachian landforms have not been extensively degraded [*Irwin and Howard*, 2002]. Here morphologic and thermal observations are used to evaluate weak materials or focused processes as alternate (or complimentary) means to explain the difference between fretted and cratered regions. In this section the material composition of different terrain types is discussed, and erosive processes are considered separately in section 4.

[12] *Malin and Edgett* [2000] have used the Mars Global Surveyor (MGS) spacecraft's Mars Orbiter Camera (MOC) to describe widespread late Noachian, friable sedimentary deposits that are susceptible to aeolian erosion, unlike highland bedrock, cratered plains materials, or more durable ancient layered deposits. In the friable deposits, yardangs and step-like exposures of subhorizontal sedimentary layers are common, but they find no evidence of fluvial erosion. The ~3–6 m boulders that are often recognized in MOC images do not occur at cliffs and talus slopes in these areas. Stripping and long-range transport of thick (hundreds of meters) deposits has occurred in these areas, presumably by wind, whereas nearby landforms in cratered materials are not deeply eroded. *Malin and Edgett* [2000] therefore suggest that these deposits disaggregate (in the modern environment) exclusively to <2–4 mm particles that are transportable by wind.

[13] The available MOC images of Aeolis Mensae fretted and knobby terrains reveal distinctive materials similar to the sedimentary deposits described by *Malin and Edgett* [2000] (Figures 4–6) except that indications of layering are rare in the fretted plateau mesas (Figures 5b and 5c). Some mesa talus surfaces are interrupted by outcrops at a few consistent levels that may represent some layering within the 2 km thickness of the mesa-forming material. Figure 4a is a Mars Odyssey Thermal Emission Imaging System (THEMIS) daytime infrared image displaying surface texture contrasts between fretted plateau materials and the adjacent highlands. At low resolution the fretted plateau surface appears smoother than the cratered plains on ~10 km spatial scales, demonstrating that middle Noachian crater topography is buried at Aeolis Mensae [*Greeley and Guest*, 1987]. At high resolution the most common features of the mesa surfaces are small, rounded knobs and irregularly shaped pits that are consistent with some aeolian deflation.

[14] The lack of obvious mesa debris on most fretted valley floors (inward of the talus) suggests that debris from the mesas could be easily removed. For example, Figure 5b shows yardangs that have developed by deflation of a thin, friable layer of possible mesa debris on a fretted valley floor. The surface exposed between (under) the yardangs has higher thermal inertia than the overlying layer and is resistant to deflation. Figure 5c shows one of two observed impact craters that are partially buried by talus. The craters may mark an unconformity between a weaker mesa-forming plateau unit and more resistant underlying materials exposed on the fretted valley floor; alternately, the craters may have formed on the fretted valley floor and were later partially buried by the back-wasting mesa. In either case the mesa appears less resistant than the fretted valley floor material. Pedestal craters occur at some locations on the fretted plateau surface and in the adjacent knobby terrain (Figure 6a), and they are common in the Medusae Fossae Formation. Pedestal craters likely form when crater ejecta armors a friable layer with coarse lag materials, protecting the underlying sediment as the friable layer is stripped around the ejecta blanket by wind [*McCauley*, 1973]. These

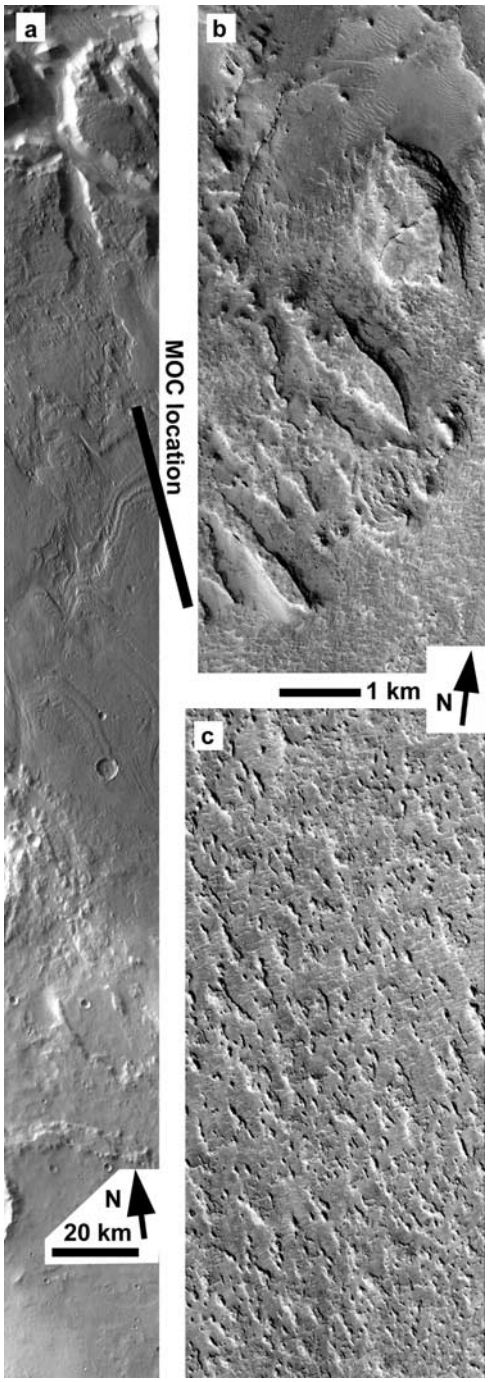

Figure 4. Deflated and etched surface of the southeastern part of the plateau, where layered sedimentary materials may overlie the massive unit in which fretted terrain has developed. (a) THEMIS image I05014001. Contrast between the etched plateau materials (north) and the underlying cratered plains (south) is shown. (b and c) MOC image E12-02859. Shown are yardangs developed in the plateau surface layers. Figure 4b is located north of Figure 4c on the image footprint.

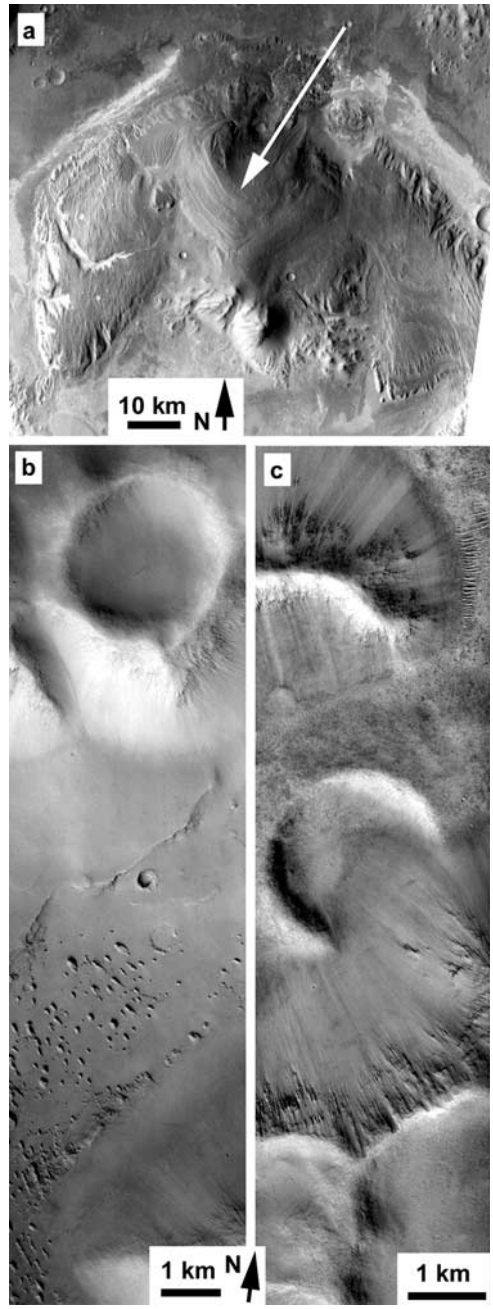

Figure 5. Layering in Gale Crater and Aeolis Mensae. (a) Layered sedimentary mound in Gale Crater, with topography shown in Figure 1. The broad, layered, lower section of the mound is overlain by a massive layer in which yardangs have developed, and the massive layers are partially overlain by a central mound of layered sediments (arrow). Figure 5a is a mosaic of THEMIS daytime IR imaging. (b) MOC image E10-02784. Shown are yardangs carved into a thin layer on a fretted valley floor, located at the northwest corner of Figure 4a. (c) MOC image E11-03930. A partially exhumed crater on a fretted valley floor from beneath talus slopes is shown.

observations demonstrate the efficacy of wind in eroding fretted plateau and knobby terrain materials, whereas unmantled cratered plains surfaces are not significantly deflated. Mainly to the southeast, parts of the plateau

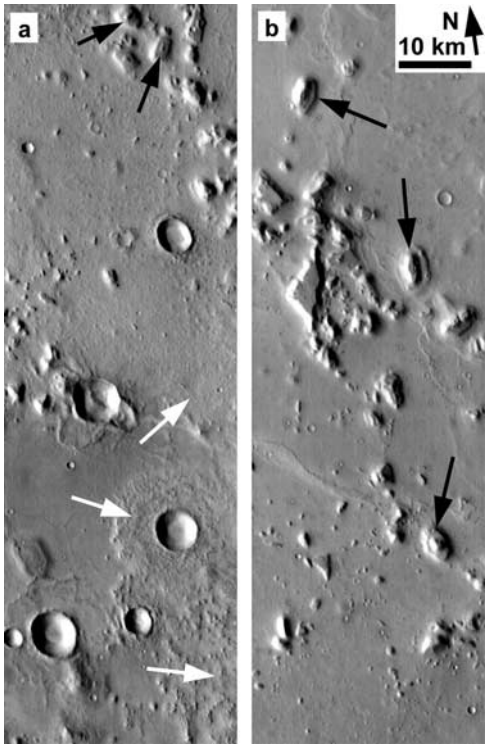

Figure 6. Pedestal craters and terraced knobs showing layered materials in knobby terrain in the western part of the study area. Black arrows indicate terraced knobs. (a) THEMIS image I01743013. White arrows indicate remnants of a layer that has been completely deflated only in the southwestern part of the image. (b) THEMIS image I01718009.

surface exhibit closely spaced, subkilometer-scale, layered knobs and yardangs that are elongated along a common primary wind direction (Figures 4b and 4c). More friable layered sediments may cap the massive fretted plateau in this area.

[15] A morphologic difference between highland bedrock and the younger, possible friable sediments is apparent in the walls of valley networks crossing the dichotomy boundary scarp. A valley has been deeply incised into crater rim materials in Figure 7a, leaving rocky outcrops and boulders in the talus (Figure 7b; see Figure 1b for topography). Figure 8a, in contrast, shows a valley that crosscuts the ~2 km boundary scarp itself, where no boulders are evident in talus. The boulder-free (at MOC resolution) talus slopes are a ubiquitous feature of mesa and fretted valley walls in Aeolis Mensae (Figures 5 and 8), whereas boulders are a common feature in cratered highland materials and terrestrial talus slopes developed from igneous rocks.

[16] The fretting process frequently crosscuts impact crater walls in the fretted plateau (Figures 2 and 3c), in contrast with impact crater rims in the adjacent highlands, which are resistant to erosion. For example, impact crater walls were the most resistant materials encountered in Ma'adim Vallis as the river was incising, whereas other materials in the cratered highlands were much less resistant to erosion (R. P. Irwin et al., Geomorphology of Ma'adim Vallis, Mars, and associated paleolake basins, submitted to *Journal of Geophysical Research*, 2004).

[17] MOC images suggest that the fretted plateau surface is somewhat cohesive or indurated. Figure 8c is a MOC image of talus slopes on a typical isolated mesa. Whereas the talus slope is nearly featureless, hummocky (but boulder-free) outcrops are common at the tops of these mesas and valley walls. Some outcrops appear at lower levels (Figure 8b). The cohesive outcrops preserve meter-scale spur-and-gully landforms or flutes, which exhibit a preferred downslope orientation toward the talus deposits, rather than alignment with a dominant wind direction. The small flutes are also visible in the valley wall crests in Figures 5c and 8, as well as many other examples in the fretted plateau, but not in valleys incised into cratered plains materials (Figure 7b). This small-scale spur-and-gully morphology is likely created by abrasion during mass wasting events, consistent with its location at the head of talus slopes. At 1 km resolution, *Mutch et al.* [1976] noted that fretted terrain slopes do not exhibit the regularly spaced wall ridges that developed by erosion of durable Valles Marineris wall rocks, but the flutes demonstrate the effectiveness of erosion by mass wasting on small spatial scales, indicating a poorly resistant material. Smaller-scale forms of this sort occur in modestly cohesive sediments, such as the damp sand and silt mixtures discussed by *Howard* [1989]. The flutes do not resemble the likely fluvial gullies common within Noachian impact craters, which are wider and deeper, display subparallel convergence patterns, and occupy nearly the entire height of the crater wall. Mesa talus slopes are generally not cratered, demonstrating that talus material has remained mobile into recent times (including when impacted by meteorites).

[18] In the knobby [*Scott and Allingham*, 1976; *Scott et al.*, 1978; *King*, 1978; *Hiller*, 1979] or undifferentiated [*Greeley and Guest*, 1987] terrains, free-standing mesas and knobs (Figures 2 and 6) are typically smaller, the knobs are more numerous, and the original surface is more densely dissected by fretted valleys where they occur. Yardangs, pedestal craters, and etched surfaces are more pervasive than in the fretted plateau. The knobby terrain also contains a number of broad, irregularly shaped, enclosed basins, which combine to form an elongated depression in the western side of the study area (arrow in Figure 1b). Fretted and knobby terrains may be composed of similar sediments, as the morphologic disparities with the adjacent cratered highland terrain also pertain to the knobby terrain in the western part of the study area. In knobby terrain the friable material was thinner or became more deeply eroded, and coarser materials were gardened from below to form the more abundant pedestal craters (Figure 6a).

[19] Gale Crater is a 150 km depression along the dichotomy boundary with a central mound of layered sediments (Figures 1, 2, and 5a), which is likely a remnant of a larger deposit that originally filled at least the crater, if not parts of the surrounding area [*Malin and Edgett*, 2000]. *Edgett and Malin* [2001] describe part of this sedimentary sequence in detail, and *Pelkey and Jakosky* [2002] and *Pelkey et al.* [2004] describe the morphology and thermophysical properties of the site. The central mound consists of (1) a relatively broad-based, layered, lower section, which occurs below the level of the crater rim (Figure 1b),

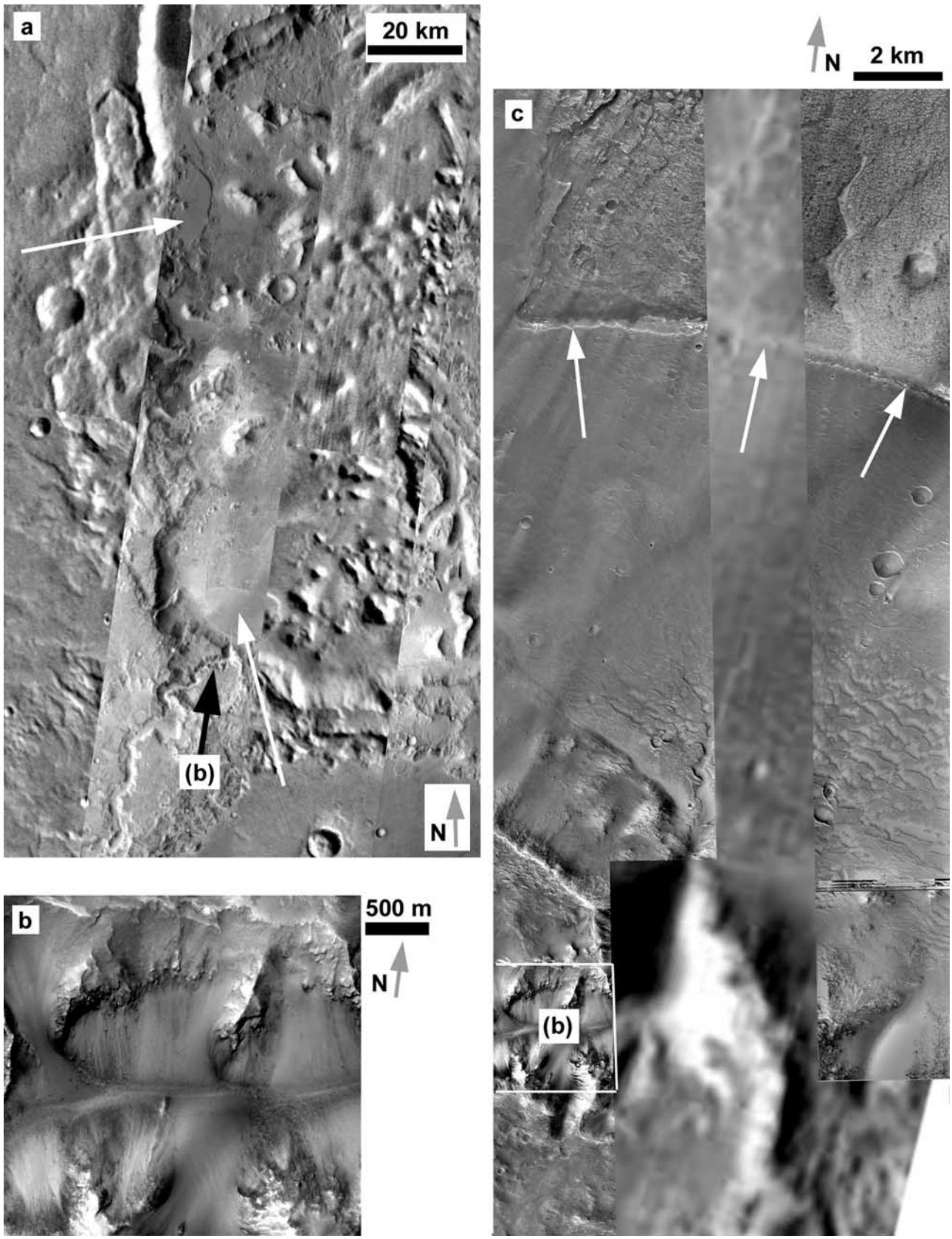

Figure 7

(2) massive middle layers, which cap the base of the mound and extend higher than the crater rim, and (3) an upper set of layered materials that superpose only the central part of the mound and extend higher than Aeolis Mensae (Figure 5a). The occurrence of the Gale mound deposits above the crater rim favors an aeolian origin for those materials, in contrast with the primarily fluvial/lacustrine deposit envisioned by *Cabrol et al.* [1999], as only the lower layered section is confined below the crater rim. The crater rim does not exhibit erosional features that would explain the elevated central mound (400 m) relative to the low northern crater rim (−2200 m). Even without modification, fresh impact craters emplaced on precursor slopes typically exhibit a downslope rim that is lower in an absolute sense than is the upslope rim.

[20] Our morphologic observations support a hypothesis that the fretted plateau is a distinct, less durable geologic material than cratered highland plains. We used the 2003 MGS Thermal Emission Spectrometer (TES) thermal inertia product [*Mellon et al.*, 2000; *Putzig et al.*, 2003] and TES-derived rock abundance data [*Nowicki and Christensen*, 1999] to determine whether the geologic materials are consistent with this hypothesis. Thermal inertia is the primary control on the amplitude of diurnal surface temperature, and the data have a formal uncertainty of ∼6% [*Mellon et al.*, 2000]. *Christensen* [1986] describes the calculation of rock abundance given multispectral infrared data, assuming a two-component surface. As natural Martian surfaces often have more than two particle size components and/or complex packing and cementation properties, the model results are only qualitatively accurate [*Pelkey and Jakosky*, 2002]. The highest thermal inertias within the fretted plateau correspond to crater floors and areas where fretted plateau materials have been partially removed, leaving widely spaced, remnant knobs (Figure 9d). The lowest thermal inertias (widespread dusty surfaces) are located in the Medusae Fossae Formation in this area. As exhumed, high thermal inertia material and younger fine-grained mantles are common in and around the fretted plateau, thermal data alone cannot provide conclusive results on the particle size of underlying geologic materials. Thermal inertia typically characterizes only the top few centimeters of the surface. These data can, however, demonstrate consistency with hypotheses that are suggested primarily by morphologic observations.

[21] We calculated the dominant grain sizes within terrain units in the study area using the 2003 thermal inertia data set [*Mellon et al.*, 2000; *Putzig et al.*, 2003], limiting our analysis to only those grid cells containing direct observations. The method is described in Appendix A. As high rock abundance can strongly influence thermal inertia values over the ∼3 km resolution of the data set, we calculated grain sizes for only those points with <10% rock abundance [*Nowicki and Christensen*, 1999]. As the median grain sizes are similar (neglecting rocks) between lowland, fretted/knobby, and highland terrains, these three terrain units are indistinguishable using these data (Table 1). The grain sizes determined for each pixel are also heterogeneous within each of these units, ranging from fine to very coarse sand. To distinguish the fretted plateau surfaces from coarser materials exposed in the fretted valley floors, we separately examined only the grain size and rock abundance data that were located entirely on the near-level tops of outlying mesas in the eastern part of the study area (Table 1). The fretted plateau surfaces show median grain sizes finer than the unmantled cratered plains, and 98% of data in this area have rock abundances <10%. These data suggest that fine-grained sediment mantles the entirety of both the Medusae Fossae and fretted plateau surfaces or that both units are composed of fine-grained sediment. We favor the latter interpretation because of the spatial consistency of the result within each unit, the efficacy of aeolian processes against both units, and the apparent morphologic homogeneity of the materials except where coarser materials have been exhumed or gardened (Figure 6). Grain size calculations from thermal inertia incorporate several sources of error, resulting in possible errors up to 50% (M. A. Presley, personal communication, 2003). The grain size calculations therefore provide only a general sense of the likely particle sizes, allowing a first-order comparison of highland and fretted plateau surfaces.

[22] The southwestern part of the cratered plains in the study area has consistently higher rock abundance, coarse grain sizes for low rock abundance pixels, and a strong spectral signature for high-Ca pyroxene and plagioclase, i.e., the basaltic surface type 1 of *Bandfield et al.* [2000] (Figures 9a and 9b). Large exposures of unmantled, unweathered basalt are not found elsewhere in the study area. The low rock abundance/low-basalt area includes the dichotomy boundary and lowland materials, but it also extends some 500 km onto the highlands (Figure 9a). This highland surface does not match either of the surface type 1 or type 2 signatures of *Bandfield et al.* [2000], but it may represent the southward extension of a thin but thermally significant dust mantle. Morphologically, the northern part of this intermediate area of cratered highlands, with low rock abundance and low-basalt signature, appears mantled or etched at meter to hundred meter resolutions (Figure 10) [*Maxwell and McGill*, 1988]. We interpret the southwestern rocky surface as unmantled cratered plains, whereas a very

Figure 7. Alluvial fans and bouldery talus developed where valleys crosscut an ancient crater rim. The features shown here postdate or are contemporaneous with erosion of interior crater sediments to form the remnant knobs. (a) Western portion of the crater, with alluvial fans indicated by white arrows, and THEMIS images over the Viking Mars Digital Image Mosaic 2.0. The black arrow shows the location of Figure 7b. (b) MOC image M18-00758. An inlet valley with bouldery outcrops and boulders in the talus is shown. (c) High-resolution view of the inlet valley (black arrow in Figure 7a) and its alluvial fan, which is well preserved with a scarp bounding the margin of the fan (white arrows). Flows did not continue into the closed basin that developed in this knobby terrain, suggesting some postfan deflation or deposition into a transient body of standing water. The scarp crest on the northern fan occurs at the same elevation (−2400 m), consistent with ponding in this enclosed basin. The white box indicates the location of Figure 7b. MOC images M18-00758, M19-02077, and E01-00870 are overlying THEMIS image I01256009.

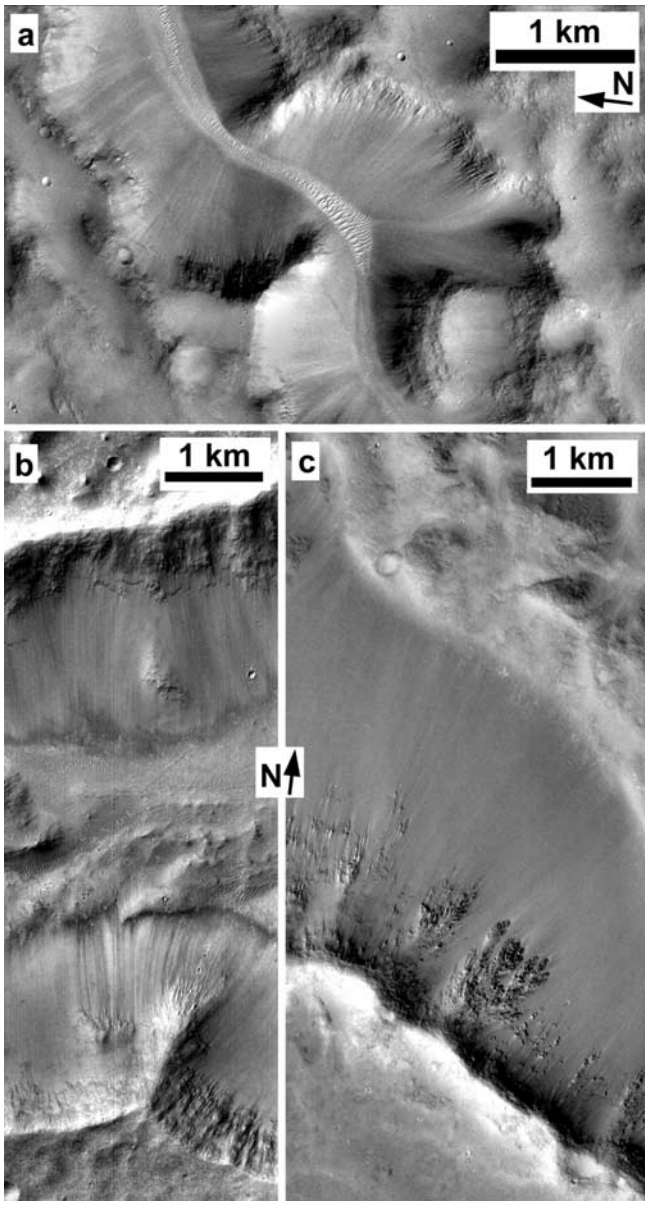

Figure 8. Similar valley crests and boulder-free talus in (a) a fluvial valley that debouched across the dichotomy boundary scarp, dissecting plateau materials, (b) sidewalls of a fretted valley with an unmantled floor, and (c) the side of an outlying isolated mesa in the fretted terrain. All observed outcrops in the fretted plateau materials have the boulder-free talus and fluted valley crests, which are not aligned with a prevailing wind direction. The strong albedo contrast at the base and crest of valley walls is an effect of high-pass filtering. Figure 8a is MOC image E10-04187, Figure 8b is MOC image M17-01198, and Figure 8c is MOC image M10-03605.

thin veneer of sedimentary material overlies cratered plains to the north, and finally a thicker fretted plateau sequence occurs along the dichotomy boundary. The Medusae Fossae surface exhibits mostly <125 μm sediments, suggesting a mantle of silt and/or dust.

[23] When interpreted with morphologic observations, the thermal inertia results suggest that the fretted plateau and knobby materials are largely a thick veneer of fine-grained sediment. Previous workers have hypothesized that plateau materials may include aeolian sediments [*Sharp*, 1973] or a poorly consolidated regolith or soil [*Squyres*, 1978; *Baskerville*, 1982], based on morphologic considerations or rapid erosion rates within the plateau. A hypothesis of coarser or more durable materials in the fretted plateau, or an extension of cratered plains materials, fails to explain this collected body of morphologic evidence and thermal measurements. The morphological and thermophysical properties of the fretted plateau are most consistent with loess [*Pye*, 1987; *Johnson and Lorenz*, 2000], which can contain a fraction of fine sand in addition to the dominant silt or dust [*Pye*, 1987]. Dunes in the region suggest that the material contains some fraction of sand or cohesive clumps of that size, although dunes are by no means ubiquitous on valley floors or mesas, nor are they necessarily derived from local materials. Terrestrial loess is also massive rather than layered, it can support near-vertical scarps, it commonly exhibits a rolling surface topography like the fretted plateau, and it can be up to hundreds of meters thick given enough time to accumulate [*Pye*, 1987]. In section 4.2 we discuss the consistency of this interpretation with the manner in which the fretted plateau and knobby terrains were degraded.

3.3. Medusae Fossae

[24] The Medusae Fossae Formation is a friable, layered material with widespread yardangs on the surface (Figure 3d). This material is thought to be Amazonian wind-transported sediments or volcanic ash [*Bradley et al.*, 2002; *Hynek et al.*, 2003] that overlies much of the dichotomy boundary region between Aeolis Mensae and Tharsis (140°–220°E). The Medusae Fossae materials onlap and sometimes surround outlying mesas of Aeolis Mensae in the northeastern part of the study area. As the controversial history and composition of Medusae Fossae have been described in detail elsewhere [*Sakimoto et al.*, 1999; *Bradley et al.*, 2002], our discussion is limited to a comparison between these deposits and the other geologic materials in the study area.

[25] Medusae Fossae is similar to the fretted plateau in that both areas appear to be friable and boulder-free, and both have low rock abundances (commonly <10%). Broad ridges >1 km high formed in both terrains above the termini of valley networks in the vicinity. In Medusae Fossae these ridges may not be entirely sedimentary but may reflect subsurface topography to some extent [*Bradley et al.*, 2002]. The overall trend of the Aeolis Mensae plateau is oriented NW–SE, subparallel to the Medusae Fossae ridges (Figure 1a). Other features of Aeolis Mensae and Medusae Fossae are significantly different. The latter is layered, poorly indurated, and has a surface dominated by relatively large yardangs [*Ward*, 1979] (Figure 3d). Medusae Fossae is also stratigraphically younger (Amazonian) and poorly cratered relative to fretted and knobby terrains. Medusae Fossae has not developed fretted terrain and mesas. The Medusae Fossae deposits serve as a proof of concept, however, that under appropriate conditions the dichotomy boundary slope has served as a site for deposition of aeolian sediments or volcanic ash. If the fretted plateau is also a fine-grained sedimentary deposit of either material, then

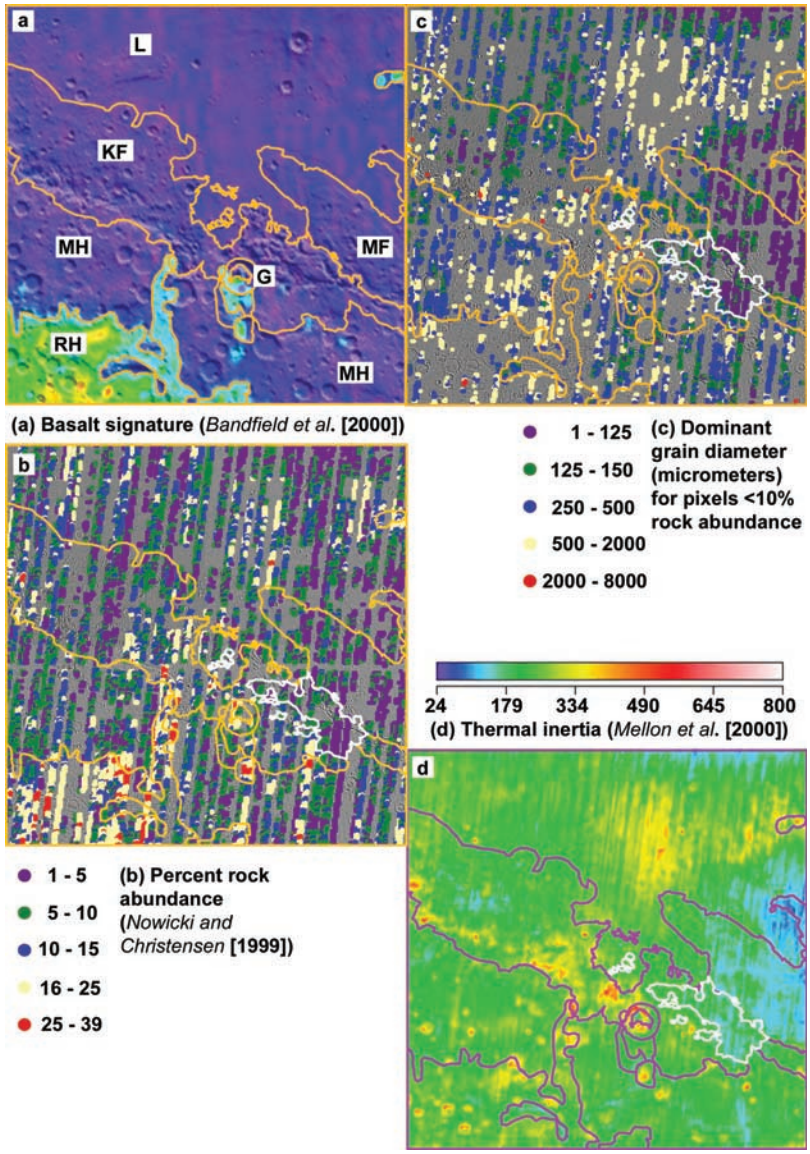

Figure 9. Features of the study area (15°N–15°S, 120°–150°E) derived from infrared measurements. Orange and purple lines are simplified unit boundaries modified from *Greeley and Guest* [1987] and based upon data from *Bandfield et al.* [2000]. White lines outline the unmodified fretted plateau surface. Boundaries are approximate. (a) Qualitative display of relative basalt abundance by *Bandfield et al.* [2000] overlaid on MOLA shaded relief. Warmer tones are stronger signatures. MF is Medusae Fossae, L is the lowlands, KF are knobby and fretted terrains, MH is the thinly mantled highlands surface, G is Gale Crater, and RH is the unmantled highland surface with strong basalt signature basalt and high rock abundance. Smaller units of RH are not labeled. (b) Percent rock abundance from *Nowicki and Christensen* [1999]. Note correspondence of rocky surfaces with stronger basalt signatures. (c) Dominant grain diameters calculated here for pixels with <10% rock abundance. Note small grain sizes over Medusae Fossae, the unmodified plateau, and parts of the adjacent lowlands. (d) Thermal inertia (J m^{-2} K^{-1} $s^{-0.5}$) from *Mellon et al.* [2000]. High thermal inertia surfaces are located in crater floors and on stripped surfaces.

multiple episodes of sedimentary deposition are expressed along the boundary.

4. Processes of Degradation

4.1. Initiating Fretted Valleys

[26] The fretted terrains lack a well-established terrestrial analog, and empirical study of these landforms is complicated by the likelihood that some portion of the geomorphic work may have occurred in the subsurface [e.g., *Lucchitta*, 1984]. The processes that affected the dichotomy boundary throughout its history must be (1) geomorphically effective on the various geologic materials and (2) consistent with processes known or inferred to have occurred on Mars contemporary with the local erosion. To conserve mass, the fretted plateau material must have been transported

Table 1. Average Values of Rock Abundance and Median Grain Size for Terrain Units in the Study Area

Terrain Unit	Rock Abundance ± Standard Deviation, %	Median Grain Size for Pixels <10% Rocks, μm
Medusae Fossae	5 ± 3	74
Lowlands	8 ± 5	274
All fretted or knobby	9 ± 5	263
Fretted plateau mesas	5 ± 2	121
Highlands, weak basalt signature	9 ± 5	364
Highlands, strong basalt signature	16 ± 7	513

either vertically or laterally to form the valleys. Alternate processes include normal faulting [*McGill and Dimitriou*, 1990]; collapse into void spaces created by subsurface dissolution, ice-related processes, intrusion, or piping [*Brook*, 1980; *Baskerville*, 1982; *Lucchitta*, 1984; *Carr*, 1996]; or surficial advective processes including aeolian, fluvial, and glacial erosion. Mass wasting may be an important corollary process but is not a reasonable means for creating subsurface void space into which material can collapse or a means for transporting sediments over distances of hundreds of kilometers out of the area. Talus slopes are generally of discrete extent and can be easily distinguished from valley floor materials (Figures 5c and 8). Near-surface processes involving ground ice are not evident in this area. We begin by addressing means by which fretted valleys could form, as carving enclosed to contiguous valleys could involve somewhat different processes than eroding isolated mesas to form smaller knobs.

[27] The irregular grid pattern of the fretted plateau mesas strongly suggests that it was initiated by fracture, at least in part [e.g., *Sharp*, 1973]. However, many of the fretted valleys are closed box canyons with steep sidewalls and are surrounded by a continuous surface of plateau materials (Figure 11), which requires that tensile stress did not significantly displace the adjacent crustal blocks. The possible fractures within fretted terrain do not appear to continue into the adjacent highlands, where faults are compressional and strike parallel to the dichotomy boundary [*Watters and Robinson*, 1999; *Watters*, 2003b]. Rather, the fretting process appears concentrated within a distinct geologic material unit. Stresses may have developed in the surface layer rather than throughout the elastic lithosphere, explaining their lack of correlation with faults in adjacent, older geologic units. Normal faulting or jointing does little

Figure 10. THEMIS images I01743013 and I04739008. (left) Dichotomy boundary with knobby terrain in the north transitioning to (right) dissected cratered plains to the south. The left frame is adjacent to and north of the right frame. North of a degraded crater (at the letter C) the northward slope breaks to a near-level surface with an etched appearance. The valley network crosscutting crater C experiences a sudden turn to the east at this site (white arrows), which likely marks the boundary of thick fretted plateau materials. South of the crater at C, depressions are better organized as linear valley networks (at letters D) that dissect sloping surfaces.

to explain the development of wide valleys, however, separating progressively smaller mesas and knobs.

[28] Some fretted valleys are contiguous with chains of closed depressions (Figure 11), both in Aeolis Mensae and north of Arabia Terra [*Baskerville*, 1982; *Lucchitta*, 1984], so collapse into void spaces may be important. Voids can be created when magma retreats from a pluton, but these chambers typically minimize surface area with respect to volume; thus the surface collapses into a rounded chamber and typically creates a circular depression on the surface. Other processes for creating voids depend on water, which can uniquely serve as a sediment transport medium in the subsurface. *Brook* [1980] proposed that ice-wedging along fractures and subsequent melting of the ice bodies might produce voids for fretted terrain, analogous to terrestrial thermokarst. He acknowledges the significant differences in scale (>100 times) between the terrestrial and Martian landforms, however. Dissolution is possible, although TES data do not suggest a favorable salt or carbonate bulk composition [*Bandfield et al.*, 2003].

[29] Piping is a tunneling process whereby water enters a mixed clay/silt/sand or volcanic ash layer, erodes the material internally, and deposits clastic sediment where the water reaches the surface again, such as at a scarp. The mechanism relies on layers of variable permeability to concentrate the flow of water. Pipes are common in terrestrial badlands, where they may be up to 3 m high and up to half as wide [*Graf*, 1988]. Expansion of the pipe ultimately results in collapse of the surface, creating a discontinuous gully, which is then widened by surface processes. Martian piping could result from discharge of highland groundwater through a fracture network in the friable fretted plateau (e.g., Figure 11a). Piping would be a reasonable process in the fretted plateau and is consistent with observations of closed fretted valleys, although the scale of fretted valleys is some 3 orders of magnitude greater than terrestrial pipes. On Mars the greater scale of some landforms may be allowed by lower gravitational stresses applied to weak materials, or perhaps some geological processes (like piping or sapping) were able to operate without competition for relatively long periods of time. The great thickness of the fretted plateau materials would support larger pipes at its base. By itself, piping does not offer a satisfactory explanation for the continued degradation of mesas to form small, dispersed knobs, separated by exposed underlying materials. It also does not offer a compelling means for isolating mesas or developing the broader enclosed basins in the western side of the study area. As the surface of the deposit is generally not dissected by fluvial gullies, the only reasonable water source for piping would be highland groundwater; yet the fretted valleys are best developed parallel to the dichotomy boundary rather than normal to it (Figure 2).

[30] Glacial erosion seems the least likely process, as none of the glacial landforms that are present on Earth (e.g., moraines, eskers) were observed in and around the fretted valleys. Furthermore, the fretted valleys have trapezoidal

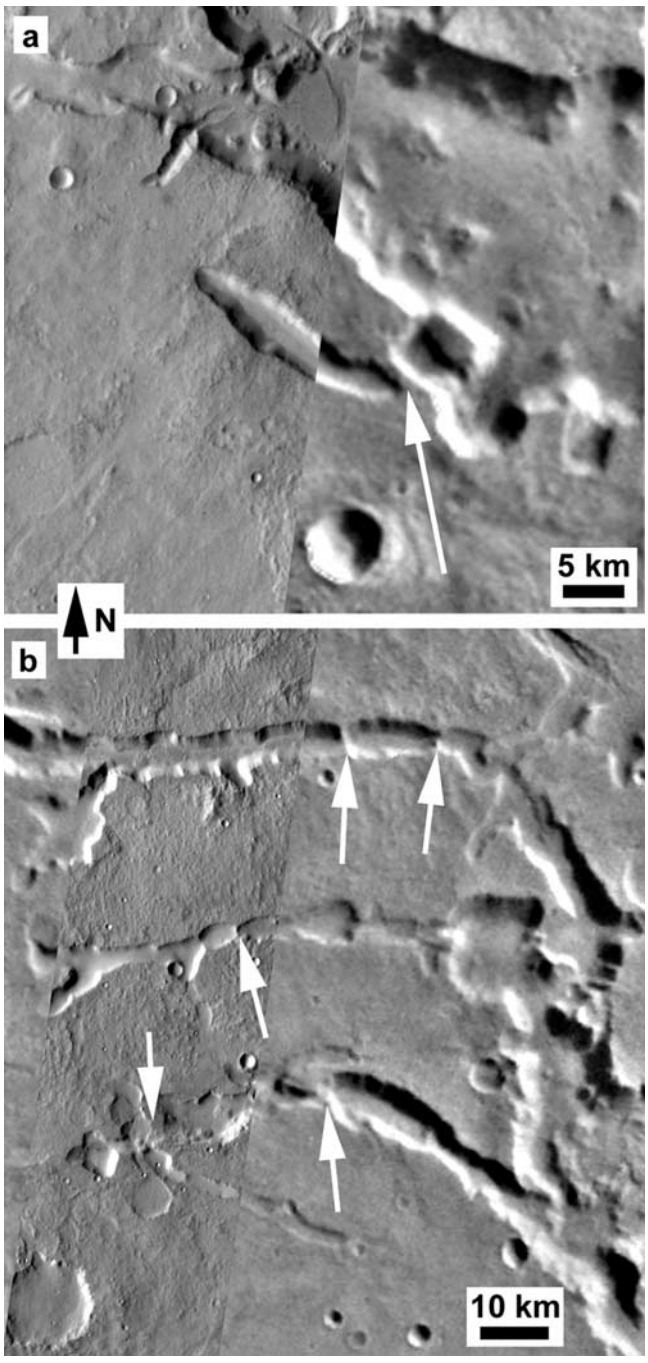

Figure 11. Fretted valleys that developed as closed depressions and have not been fully integrated. White arrows indicate continuous plateau surfaces that isolate the depressions. (a) THEMIS image I01418005 overlaid on the Viking MDIM 2.0. An elongated depression is the southernmost fretted valley in the immediate vicinity before the southward transition to cratered plains. Although the scene is only 70 km east of Gale Crater, the surface is not mantled by ejecta, suggesting that the Aeolis Mensae fretted plateau overlies Gale ejecta or that the ejecta has been eroded or degraded. This stratigraphic relationship is contrary to the sequence mapped by *Greeley and Guest* [1987] based on Viking imaging. (b) THEMIS image I01705005 overlaid on the Viking MDIM 2.0. Several closed depressions form a sausage-link pattern in these fretted valleys. Note the knobby texture of the fretted plateau surface at 100 m/pixel resolution.

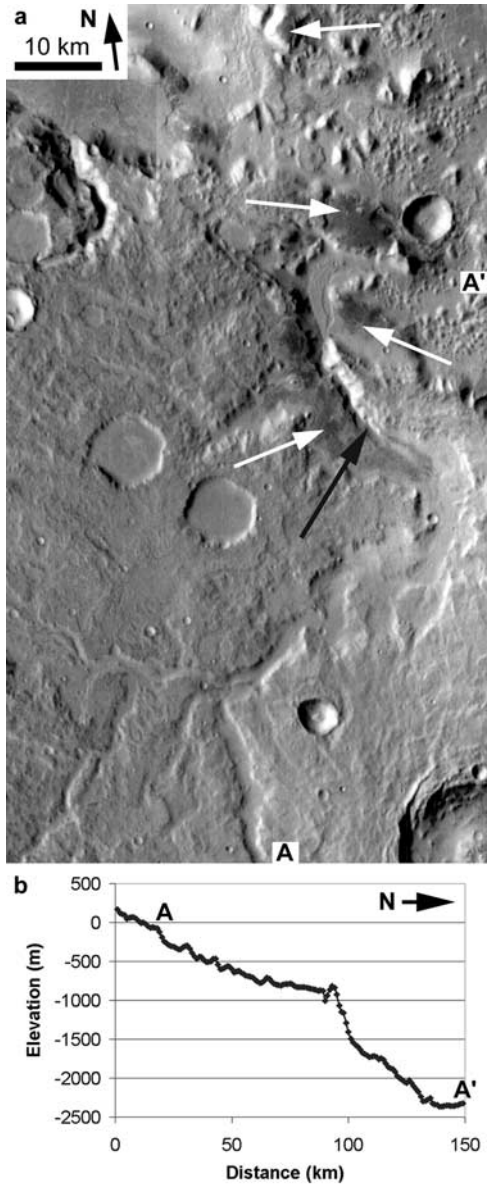

Figure 12. Valley networks crossing the dichotomy boundary scarp, exhibiting abrupt base-level declines. (a) Mosaic of THEMIS images I02367004, I02005008, and I01306006. The valley in the northwest corner of the image is the valley in Figure 8a. To the eastern side of this image, a valley developed a broad, flat plain with a −900 m base level, which is presently armored by relatively coarse materials (thermally dark in the daytime, indicated by white arrows). Some outlying mesas are also armored with this coarse material. Development of knobby terrain to the north caused a base-level decline to −2300 m and development of a knickpoint in the longitudinal profile (black arrow). (b) Longitudinal profile of the eastern valley in Figure 12a. Note that north is to the right.

rather than U-shaped cross-sections, glaciers do not form enclosed scarp-bounded depressions in plateaus, and the irregular gridded pattern of the mesas seems inconsistent with any preferred glacial transport direction.

[31] The pattern of mesas and the presence of closed depressions also pertain to surface fluvial erosion. *Breed et al.* [1982] used Egyptian desert analogs to explain fretted terrain by fluvial erosion and scarp retreat, followed by aeolian erosion of remnant mesas in an increasingly arid climate. Fretted valleys in Aeolis Mensae also completely encircle knobs, but any flow path in the present surface would require crossing enclosed basins within the fretted terrain, and the spatial pattern of fretted valleys (Figure 2) does not resemble any of the convergent flow patterns that are characteristic of fluvial valleys on either Earth or Mars (e.g., Figure 12a). We have not observed channels on fretted valley floors, although they do occur in some highland valley networks. The mesa slopes in Aeolis Mensae are not dissected by deep gullies but exhibit near-linear scarps, in contrast with Noachian crater rims in the adjacent highlands. Therefore any possible fluvial erosion of the mesas by runoff must have been completely masked by later significant, nonfluvial degradation, except along the boundary with cratered terrain, where a few fluvial valleys are evident. Some limited fluvial erosion could be responsible for initiating some of the branch valleys in fretted terrain, as several of these are connected with highland valley networks rather than originating in chains of closed depressions.

[32] The crosscutting of some valley networks into the fretted terrain (Figures 7 and 12) suggests that at least one limited episode of highland fluvial activity occurred after the fretted valleys formed. Longitudinal profiles of these valley networks steepen abruptly as they cross the boundary scarp, which suggests that channels had little time to regrade after the fretted terrain development imparted a base-level decline to the north. A more mature channel will develop a straight to concave-up (well-graded) longitudinal profile [*Davis*, 1902] with a declining gradient as the channel approaches its terminal base level. In Figure 12 a valley network had established a well-graded profile with a broad lower reach. Base-level decline, associated with development of an enclosed basin in the knobby terrain (Figure 1) and a southward advancement of the boundary scarp [*Irwin and Howard*, 2002], resulted in incision of a canyon into the lower valley floor. These valley networks do not continue through the fretted terrain but terminate at alluvial fans or fan deltas in closed depressions along the dichotomy boundary (Figure 7), and no flow paths are available through closed basins in the fretted terrain (Figure 1). Although resistant outcrops can be responsible for steep lower reaches, such outcrops were not observed at the crosscutting valley walls (Figure 8a), except where a valley was incised into buried crater rim materials (Figure 7). If the valleys were frequently active during the development of fretted terrain, ample time would be available for some base-level compensation.

[33] As none of the above mechanisms seems satisfactory by itself, particularly those involving runoff, wind must be examined as either a primary erosive process or one that could support another mechanism. Dunes are commonly transverse to the long axis of fretted valleys, regardless of a valley's orientation, demonstrating that aeolian sediment transport within the fretted valleys is dominated by local wind conditions rather than a regional prevailing wind. Yardangs with variable orientations in the Medusae Fossae

also suggest that the prevailing wind has varied with time in the region [*Wells and Zimbelman*, 1997; *Bradley et al.*, 2002], so reliance on the modern prevailing wind to erode the valleys is not necessary. As it operates primarily along the long axis of the valleys, wind possibly could extend a fretted valley headward once the plateau surface was breached. The main issue with aeolian erosion is its ability to establish elongated valleys or chains of depressions in the first place, while doing relatively little geomorphic work on the surrounding upland surface. Development of fretted valleys by wind in the plateau would benefit greatly from a small impact, collapse pit, or fracture, which would breach the indurated surface and provide a site where wind could attack weaker underlying material. Once the fretted valley is initiated as an alcove in a crater, funneling of wind into that alcove could support its headward growth.

[34] In summary, initiation of the fretting process (i.e., development of the valleys prior to degradation of mesas to form knobs) is a complex issue, which may involve two or more complementary processes. To explain the linear chains of scarp-bounded, closed depressions in fretted terrains and the absence of reasonable evidence for surface flows, one possible mechanism for initiating fretted valleys includes the following sequence: (1) fracture, (2) possible piping or subsurface processes involving ice at the base of the fretted plateau materials, (3) collapse into void spaces or small impacts to breach the indurated plateau surface, and (4) significant aeolian deflation. Fine-grained sediment such as loess would be an ideal candidate material where these processes could be highly effective over timescales on the order of $\sim 10^8$ years. In section 4.2 we discuss the influence of weathering on this early stage and in the continued development of fretted terrain.

4.2. Weathering-Limited Scarp Retreat

[35] None of the processes for initiating discontinuous collapse pits or small fretted valleys (i.e., piping, ice melt, impacts, or fluvial erosion, exploiting a spatially confined fracture system) explains the wholesale degradation of mesas to knobs and the development of closed, irregularly shaped depressions. In his initial study of fretted terrain, *Sharp* [1973] used ~1 km/pixel Mariner 9 data to conclude that scarp retreat was the most likely mechanism for the development of fretted terrain, owing to the prevalence of talus slopes bounding the isolated mesas. If the shear strength of a weak material is exceeded by the vertical gravitational stress, a scarp will fail and develop a talus slope at the angle of repose (~30°). In weak materials, removal of material from the talus only encourages further slope failures, and a cliff never develops. *Sharp* [1973] examined possible mechanisms for scarp retreat involving groundwater or ground ice, noting that layered volcanic or aeolian materials of differential resistance were ideal candidates for the fretted terrain parent rocks. We have shown that the fretted plateau materials are friable and bounded by boulder-free talus slopes, so basalt or similar durable rocks can be ruled out.

[36] Following incision, impact, or collapse, an initial small valley in friable materials offers fresh slopes where mass wasting can occur. At this stage, given a fluid medium (air or water) that can transport sediment from talus slopes out of the area, slopes in the friable fretted plateau should continue to fail, the valley should widen and/or extend headward, and mesas should ultimately degrade to smaller knobs. In this scheme, degradation of friable mesas to knobs requires only a long-range transport process that could remove materials out of the area over distances of hundreds of kilometers. Given that, the degradation would be naturally self-perpetuating and limited only by the transport capacity of the eroding medium. *Sharp* [1973] suggested that the transport was accomplished by wind. However, the somewhat indurated plateau materials (particularly the cap) are not expected to completely disaggregate back to sand or smaller particles during a slope failure, but some small clumps of material would remain and form a lag to resist aeolian deflation. If the transport process were not immediately capable of transporting talus materials, then the erosion of mesas would be limited by the weathering rate.

[37] A weathering-limited slope retreat process may solve the question of why the fretting process would largely end in the early Hesperian [*Neukum and Hiller*, 1981; *Maxwell and McGill*, 1988; *McGill*, 2000]. For the fretting process and degradation of mesas to end, either the transport rate or the weathering (disaggregation) rate, both on the surface and along subsurface joints, must have declined dramatically during the Hesperian. In addition to intergranular attractive forces, terrestrial loess is initially cemented by influx of water from precipitation, which recrystallizes easily dissolved components (salts, carbonates) to cement the matrix materials (silicates). A small amount of cementation allows loess to stand in steep bluffs because of the fine grain size and large contact area/grain volume ratio. Subsequent leaching of the cement (in terrestrial situations mostly below the water table) disaggregates the deposit and allows mass wasting and ready erosion [*Pye*, 1987]. Small amounts of water may have been supplied by limited frost deposition and melting during the Hesperian. Alternately, groundwater may have seeped to the surface at the base of the knobs or in the fretted valleys in the past before evaporating or freezing [*Howard*, 1991]. A limited volume of water may have been delivered to the fretted and knobby terrains by intermittent discharge of highland valley networks, as some of them crosscut the dichotomy scarp (Figures 7, 8, 10, and 12). The decline in erosion rates suggests that the weathering process declined during the early Hesperian, which is coincident with the general decline of aqueous processes on Mars [*Carr*, 1996].

[38] As an alternate possibility, fragments of loess could be weathered by impact of saltating sand-sized particles derived from the highlands or from underlying coarse layers. Such particles would preferentially abrade the base of the talus slopes and knobs without affecting the crests, whereas higher surfaces would be modified only directly by wind. *Manent and El-Baz* [1986] suggested that large Martian knobs had been elongated by aeolian processes. Aeolian erosion rates may have also declined during the Hesperian with a thinning atmosphere. Without a more robust weathering process, aeolian riving (disaggregation) would work at a similar rate on the talus slopes as on the flat mesa tops, which have both experienced little erosion beyond the late Noachian to early Hesperian.

4.3. Long-Range Transport Processes

[39] As glacial landforms are not evident, water and wind are the most likely long-range transport processes given the

diverse available evidence for their presence and activity on Mars [e.g., *Baker*, 1982; *Greeley and Iversen*, 1985; *Carr*, 1996; *Malin and Edgett*, 2001]. Owing to the lack of observed valley networks, lack of reasonable flow paths, lack of deep gullies incised into steep slopes, and poor grading of highland networks to lowland base levels, large-scale erosion of the boundary sedimentary deposits by water is unlikely. In contrast, evidence of aeolian erosion is pervasive, including etched terrain (Figures 4, 5, 6, and 10), dunes (Figures 4b and 4c), yardangs (Figures 4 and 5), and closed basins (Figures 1 and 11) with no obvious alternate formative process. Wind on Mars has been long-lived and ubiquitous. Although we have not observed reasonable relict flow paths or other evidence for extensive surface fluvial erosion of the fretted plateau, in principle, fluvial erosion could have transported sedimentary materials away from talus slopes at other areas on Mars [*Breed et al.*, 1982], supporting a transport-limited slope retreat process. Neither aeolian nor fluvial processes can be excluded on a global scale based only on this study area. Generally, fretted terrain is connected with large, sinuous valley networks more commonly in Arabia Terra [*Carr*, 2001] than at Aeolis Mensae.

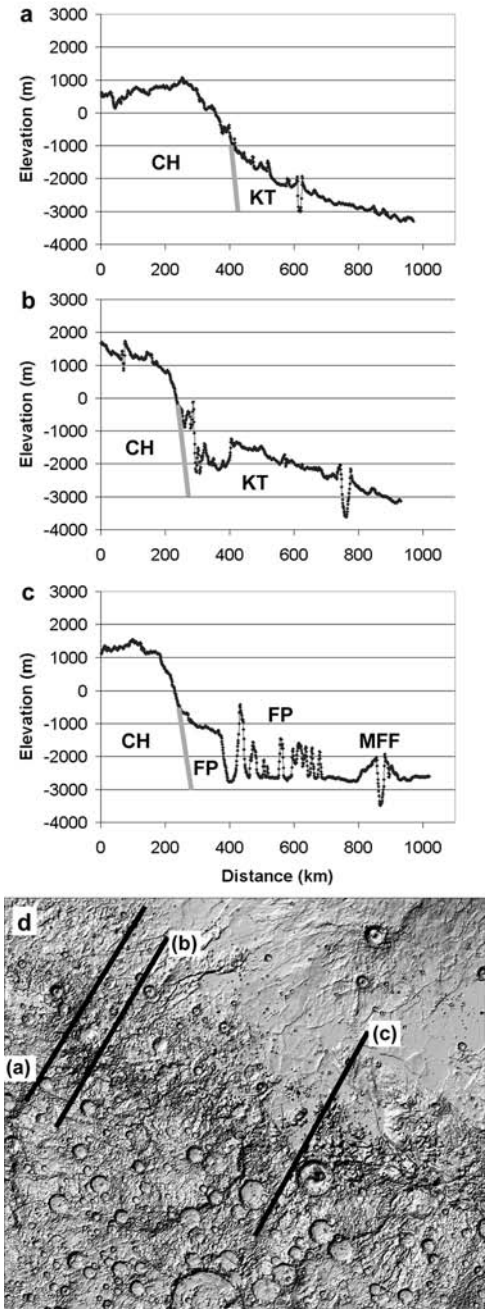

Figure 13. Topographic profiles across the dichotomy boundary in the study area, showing the approximate location of a precursor dichotomy boundary slope (gray lines) along which sediments were deposited. To the south (left) are the high-standing cratered highlands (CH), and topography of the knobby terrain (KT), fretted plateau (FP), and Medusae Fossae Formation (MFF) are shown to the north. The break in slope at about −1000 m corresponds to the southern extent of sedimentary materials identified from surface morphology. (a) A shallow, northward declining slope largely preserved in the knobby terrain. (b) A trough excavated from the knobby terrain deposit. However, initial topography of the deposit is preserved on both sides of the trough. (c) The fretted plateau deposit, which has been eroded to form larger mesas. (d) MOLA shaded relief map showing the locations of topographic profiles (bounded by 15°N, 15°S, 115°E, and 150°E).

5. Discussion and Conclusions

[40] Morphologic and thermal observations suggest that Aeolis Mensae fretted plateau mesas are composed of a friable sedimentary material, which differs compositionally from the older highland cratered plains materials but may resemble the younger Medusae Fossae sediments. The fretted deposits have boulder-free talus at MOC resolution, small-scale spur-and-gully morphology, massive and layered stratigraphic units, knobs and yardangs, a near absence of fluvial valleys, and they overlie the termini of some valley networks in the area. The fretted materials supported high erosion rates on the order of 10^{-2} mm year^{-1} within fretted valleys, which formed only in materials with these morphologic characteristics. Fretted valleys indiscriminately breached crater rims in the plateau materials, but the rims are resistant to erosion when developed in the adjacent highland rocks. The fretted plateau deposits have thermal properties and rock abundances that suggest a well-sorted deposit of fine sand and smaller grains, which overlie coarser materials that are exposed at stripped surfaces and in impact ejecta.

[41] The late Noachian fretted plateau materials bury an early to middle Noachian dichotomy boundary slope (Figure 13), which was heavily modified by cratering and fluvial erosion prior to deposition of the plateau sediments. After the fretting process ended by the middle of the Hesperian period, smooth plains associated with Elysium Mons embayed the fretted plateau and knobby terrains. Medusae Fossae layered air fall deposits [*Bradley et al.*, 2002] postdate all other major geologic units in the study area.

[42] Aeolian and (less significant) fluvial processes may have been responsible for emplacement of the fretted

plateau deposit, but observed aeolian deflation sites and pedestal craters require that the sediments were very well sorted, with no major lag-forming component of granules (2–4 mm) or larger particles that would not be transportable by wind [*Greeley and Iversen*, 1985]. Whereas wind is a capable mechanism for sorting these particles, valley networks would probably deliver some coarse materials that would form a lag during deflation. For example, some channels delivered coarse sediment to terminal alluvial fans as they incised into bedrock along the boundary (Figure 7). These fans have remained well preserved as the particles were not transportable by wind. The valley network in Figure 12 also delivered coarse (thermally dark in daytime infrared) sediments onto its own broad valley floor and onto the fretted and knobby terrain deposit, where the fluvial materials now serve as a capping lag for outlying mesas. Given few examples of fluvial valleys interacting with the fretted plateau deposit, it appears to have been emplaced mainly by wind.

[43] The confinement of the well-sorted deposit as a discrete sedimentary wedge along the older dichotomy boundary suggests emplacement primarily by aeolian processes from lowland sediment sources. The adjacent highlands retain widespread, well-preserved ~20–50 m deep valley networks and small craters, suggesting that these depressions have experienced little aeolian resurfacing since the end of intense crater degradation [*Irwin and Howard*, 2002]. As such, the highlands are likely not the source area for this deposit. An easterly wind would be expected to lose velocity in a low-lying band at the base of the dichotomy boundary, possibly favoring sediment deposition there, and velocity would increase again as the air moved upslope [*Walmsey et al.*, 1982; *Taylor et al.*, 1987]. Other conditions favoring sediment deposition are possible, and the Medusae Fossae deposits confirm that the dichotomy boundary has been a sediment trap at times in the past. Wind direction and speed appear to have varied over time, as modern global convection model results are inconsistent with relict yardang orientations [*Greeley et al.*, 1993]. Moreover, yardangs in the Medusae Fossae commonly have more than one orientation within the unit [*Wells and Zimbelman*, 1997; *Bradley et al.*, 2002]. Aeolis Mensae deposits reach variable elevations above −1000 m, higher than the older valley network termini in the region, so origin as a marine deposit is also unlikely.

[44] The timing of this emplacement is relevant to the possibility of a northern sea on Mars [*Parker et al.*, 1989, 1993; *Clifford and Parker*, 2001; *Carr and Head*, 2003], as any possible Noachian shoreline has been obscured in this area by ~2 km thick deposits. If such a water body supplied Noachian valley networks through evaporation and precipitation, gradual recession of the ocean might simultaneously expose sediments for aeolian transport and reduce water supply to the valley networks. These were contemporary events in this area, which provide one speculative possibility for the sediment source. Another is volcanic ash, which might have been produced at Elysium Mons, Apollinaris Patera, or other volcanoes and might have been transported into this area by wind. Previous studies have shown that the northern lowland is a natural sediment trap [e.g., *Soderblom et al.*, 1973; *Lucchitta et al.*, 1986; *Tanaka et al.*, 2003], which could have provided sediment to Aeolis Mensae from other sites. Present data do not allow us to distinguish between these sediment sources with certainty, although the fretted plateau appears older than the outflow channels and polar deposits. The fretted terrain materials are similar to the younger Medusae Fossae Formation in that both appear to be fine-grained sedimentary deposits, but the somewhat cemented or otherwise indurated fretted plateau resisted aeolian erosion except where compromised, yielding a very different landscape in the older fretted deposit.

[45] Fretted terrain is well preserved in this area, as Amazonian debris aprons and lineated valley fill, which have been suggested as evidence for ground ice in Arabia Terra [e.g., *Squyres*, 1978], do not characterize the fretting process in Aeolis Mensae. Fretting began with establishment of a fracture system in the plateau materials, followed possibly by collapse into void spaces or impacts to compromise the durable surface of the unit. Voids could have been produced by piping or intrusion of water followed by freezing and ice melt [*Brook*, 1980]. Disaggregation of the mass wasted debris reduced it again to small particles, which were largely transported out of the region by wind. The friable nature of the fretted plateau materials left the talus more susceptible to weathering by small amounts of water or impact of windborne-saltating particles relative to adjacent cratered plains materials that include coarse ejecta. Aeolian scour of these small fault, impact, or collapse depressions would exploit coincident fracture traces, lengthening the valleys primarily along an easterly to southeasterly wind direction and its aligned fractures. Once initiated, fretted valleys channeled wind down the length of the valley rather than relying on the prevailing wind, as demonstrated by modern dune orientations. As talus materials were transported away, slopes continued to fail to restore the talus gradient and minimize scarp heights, so the mesas were degraded to knobs primarily by weathering-limited scarp retreat. The fretting process declined after operating on the order of $\sim 10^8$ years [*Neukum and Hiller*, 1981] with lower weathering and sediment transport rates in the early Hesperian, although some erosion of the surface continues to the present. Fresh talus slopes and wind-eroded knobs are common in the area.

[46] Major depositional and geomorphic events in this area can be summarized as follows: (1) middle and late Noachian: cratering and erosion of the precursor dichotomy boundary contemporary with and similar to cratered highland degradation, (2) near late Noachian/Hesperian boundary: emplacement of fretted plateau materials as an aeolian sedimentary wedge, probably from lowland sources, and induration of the surface and fracture of the deposit, (3) contemporary into early Hesperian: fretting process exploiting craters, faults, and possible collapse pits formed by ice melt or piping; aeolian riving and possible aqueous weathering disaggregating sedimentary particles from talus, followed by aeolian transport of sedimentary materials out of the region; steepening of talus slopes supporting scarp retreat of mesas by mass wasting; and limited fluvial erosion of the highland boundary occurring during the last stage of valley network activity, and (4) Amazonian: emplacement of Elysium smooth plains and Medusae Fossae.

[47] These observations reveal an important depositional and geomorphic event along this part of the dichotomy

boundary, which explains how fretted terrain could develop there and not in adjacent highland materials. Although the global extent of these deposits has not yet been determined, observations in this study area may provide clues to why the more ancient valley networks and younger fretted terrains appear concentrated in discrete regions.

Appendix A: Calculation of Grain Size From Thermal Inertia

[48] Thermal inertia I (J m^{-2} K^{-1} s$^{-0.5}$) is defined as

$$I \equiv \sqrt{\kappa \rho c}, \tag{A1}$$

where κ is thermal conductivity (J s^{-1} m^{-1} K^{-1}), ρ is bulk density (kg m^{-3}), and c is heat capacity (J kg^{-1} K^{-1}). *Mellon et al.* [2000] held ρ and c constant at 1500 and 627.9, respectively, so κ can be determined from the thermal inertia. The dominant grain size d (μm) of the material is calculated from κ using the relationship given by *Presley and Christensen* [1997]:

$$d = \left(\kappa / CP^{0.6}\right)^{X}, \tag{A2}$$

where P is atmospheric pressure (torr), $X = (-0.11 \log P/K)^{-1} \approx 0.5$, and C and K are constants ($C = 0.0015$ and $K = 8.1 \times 10^4$ torr). P was calculated from the elevation of the surface, given by the MOLA 128 pixel/degree model and the relationship

$$P = P_r \exp\left(-zH_r^{-1}\right), \tag{A3}$$

where z is elevation (m) above the isobar of the constant reference pressure P_r (6.1 mbar = 4.6 torr on Mars), and H_r is a constant atmospheric scale height (taken to be 10 km for Mars [*Zurek et al.*, 1992]). In MOLA topography the 6.1 mbar isobar occurs at approximately −1600 m elevation [*Smith et al.*, 2001].

[49] **Acknowledgments.** We gratefully acknowledge our dialogue with M. Presley and the thermal inertia, rock abundance, and qualitative basalt abundance data sets provided to the community by M. Mellon, P. Christensen, and J. Bandfield, respectively. We appreciate the helpful comments of J. Plescia and an anonymous reviewer. This research was supported by a NASA Mars Data Analysis Program grant to T. Watters.

References

Baker, V. R. (1982), *The Channels of Mars*, 198 pp., Univ. of Tex. Press, Austin.

Bandfield, J. L., V. E. Hamilton, and P. R. Christensen (2000), A global view of Martian surface compositions from MGS-TES, *Science*, *287*, 1626–1630.

Bandfield, J. L., T. D. Glotch, and P. R. Christensen (2003), Spectroscopic identification of carbonate minerals in the Martian dust, *Science*, *301*, 1084–1087.

Bartley, W. W. (1964), Rationality versus the theory of rationality, in *The Critical Approach to Science and Philosophy*, edited by M. Bunge, pp. 3–31, Free Press, New York.

Baskerville, C. A. (1982), Collapse: A mechanism for martian scarp retreat, in *Reports of the Planetary Geology Program*, *NASA Tech. Memo., 85127*, 244–252.

Bradley, B. A., S. E. H. Sakimoto, H. Frey, and J. R. Zimbelman (2002), Medusae Fossae Formation: New perspectives from Mars Global Surveyor, *J. Geophys. Res.*, *107*(E8), 5058, doi:10.1029/2001JE001537.

Breed, C. S., J. F. McCauley, and M. J. Grolier (1982), Relict drainages, conical hills, and the eolian veneer in southwest Egypt: Applications to Mars, *J. Geophys. Res.*, *87*, 9929–9950.

Brook, G. A. (1980), The Martian fretted terrains: Examples of thermokarst labyrinth topography, in *Reports of the Planetary Geology Program*, *NASA Tech. Memo., 82385*, 369–372.

Cabrol, N. A., E. A. Grin, H. E. Newsom, R. Landheim, and C. P. McKay (1999), Hydrogeologic evolution of Gale Crater and its relevance to the exobiological exploration of Mars, *Icarus*, *139*, 235–245.

Carr, M. H. (1996), *Water on Mars*, 229 pp., Oxford Univ. Press, New York.

Carr, M. H. (2001), Mars Global Surveyor observations of Martian fretted terrain, *J. Geophys. Res.*, *106*, 23,571–23,593.

Carr, M. H., and J. W. Head III (2003), Oceans on Mars: An assessment of the observational evidence and possible fate, *J. Geophys. Res.*, *108*(E5), 5042, doi:10.1029/2002JE001963.

Christensen, P. R. (1986), The spatial distribution of rocks on Mars, *Icarus*, *68*, 217–238.

Clifford, S. M., and T. J. Parker (2001), The evolution of the Martian hydrosphere: Implications for the fate of a primordial ocean and the current state of the northern plains, *Icarus*, *154*, 40–79.

Craddock, R. A., and T. A. Maxwell (1990), Resurfacing of the Martian highlands in the Amenthes and Tyrrhena region, *J. Geophys. Res.*, *95*, 14,265–14,278.

Craddock, R. A., and T. A. Maxwell (1993), Geomorphic evolution of the Martian highlands through ancient fluvial processes, *J. Geophys. Res.*, *98*, 3453–3468.

Craddock, R. A., T. A. Maxwell, and A. D. Howard (1997), Crater morphometry and modification in the Sinus Sabaeus and Margaritifer Sinus regions of Mars, *J. Geophys. Res.*, *102*, 13,321–13,340.

Davies, G. F., and R. E. Arvidson (1981), Martian thermal history, core segregation, and tectonics, *Icarus*, *45*, 339–346.

Davis, W. M. (1902), Base-level, grade, and peneplain, *J. Geol.*, *10*, 77–111.

Edgett, K. S., and M. C. Malin (2001), Rock stratigraphy in Gale Crater, Mars, *Proc. Lunar Planet. Sci. Conf.*, *32*, 1005.

Frey, H. V., and R. A. Schultz (1988), Large impact basins and the mega-impact origin for the crustal dichotomy on Mars, *Geophys. Res. Lett.*, *15*, 229–232.

Frey, H. V., and R. A. Schultz (1990), Speculations on the origin and evolution of the Utopia-Elysium lowlands of Mars, *J. Geophys. Res.*, *95*, 14,203–14,213.

Frey, H. V., J. H. Roark, K. M. Shockey, E. L. Frey, and S. E. H. Sakimoto (2002), Ancient lowlands on Mars, *Geophys. Res. Lett.*, *29*(10), 1384, doi:10.1029/2001GL013832.

Graf, W. L. (1988), *Fluvial Processes in Dryland Rivers*, 346 pp., Blackburn Press, Caldwell, N. J.

Greeley, R., and J. E. Guest (1987), Geologic map of the eastern equatorial region of Mars, *U.S. Geol. Surv. Map, I-1802-B*.

Greeley, R., and J. D. Iversen (1985), *Wind as a Geological Process*, 333 pp., Cambridge Univ. Press, New York.

Greeley, R., A. Skypeck, and J. B. Pollack (1993), Martian aeolian features and deposits: Comparisons with general circulation model results, *J. Geophys. Res.*, *98*, 3183–3196.

Guest, J. E., P. S. Butterworth, and R. Greeley (1977), Geological observations in the Cydonia region of Mars from Viking, *J. Geophys. Res.*, *82*, 4111–4120.

Hartmann, W. K., and G. Neukum (2001), Cratering chronology and the evolution of Mars, *Space Sci. Rev.*, *96*, 165–194.

Hiller, K. H. (1979), Geologic map of the Amenthes quadrangle of Mars, *U.S. Geol. Surv. Map, I-1110 (MC-14)*.

Howard, A. D. (1989), Miniature analog of spur-and-gully landforms in Valles Marineris, in *Reports of the Planetary Geology and Geophysics Program–1988*, *NASA Tech. Memo., 4130*, 355–357.

Howard, A. D. (1991), Role of artesian groundwater in forming martian permafrost features, in *Reports of the Planetary Geology and Geophysics Program-1990*, *NASA Tech. Memo., 4300*, 120–122.

Hynek, B. M., R. J. Phillips, and R. E. Arvidson (2003), Explosive volcanism in the Tharsis region: Global evidence in the Martian geologic record, *J. Geophys. Res.*, *108*(E9), 5111, doi:10.1029/2003JE002062.

Irwin, R. P., III, and A. D. Howard (2002), Drainage basin evolution in Noachian Terra Cimmeria, Mars, *J. Geophys. Res.*, *107*(E7), 5056, doi:10.1029/2001JE001818.

Janle, P. (1983), Bouguer gravity profiles across the highland-lowland escarpment on Mars, *Moon Planets*, *28*, 55–67.

Johnson, J. B., and R. D. Lorenz (2000), Thermophysical properties of Alaskan loess: An analog material for the Martian polar layered terrain?, *Geophys. Res. Lett.*, *27*, 2769–2772.

King, E. A. (1978), Geologic map of the Mare Tyrrhenum quadrangle of Mars, *U.S. Geol. Surv. Map, I-1073 (MC-22)*.

Lanz, J. K., R. Hebenstreit, and R. Jaumann (2000), Martian channels and their geomorphologic development as revealed by MOLA, paper presented at Second International Conference on Mars Polar Science

and Exploration, Lunar and Planet. Inst., Reykjavik, Iceland, 21–25 Aug.
Lingenfelter, R. E., and G. Schubert (1973), Evidence for convection in planetary interiors from first-order topography, *Moon*, *7*, 172–180.
Lucchitta, B. K. (1984), Ice and debris in the fretted terrain, Mars, *J. Geophys. Res.*, *89*, B409–B418.
Lucchitta, B. K., H. M. Ferguson, and C. Summers (1986), Sedimentary deposits in the northern lowland plains, Mars, *J. Geophys. Res.*, *91*, E166–E174.
Malin, M. C., and K. S. Edgett (2000), Sedimentary rocks of early Mars, *Science*, *290*, 1927–1937.
Malin, M. C., and K. S. Edgett (2001), Mars Global Surveyor Mars Orbiter Camera: Interplanetary cruise through primary mission, *J. Geophys. Res.*, *106*, 23,429–23,570.
Manent, L. S., and F. El-Baz (1986), Comparison of knobs on Mars to isolated hills in eolian, fluvial and glacial environments, *Earth Moon Planets*, *34*, 149–167.
Mangold, N. (2000), Crater density of lobate debris aprons and fretted channels: Paleoclimatic implications, paper presented at Second International Conference on Mars Polar Science and Exploration, Lunar and Planet. Inst., Reykjavik, Iceland, 21–25 Aug.
Mangold, N. (2003), Geomorphic analysis of lobate debris aprons on Mars at Mars Orbiter Camera scale: Evidence for ice sublimation initiated by fractures, *J. Geophys. Res.*, *108*(E4), 8021, doi:10.1029/2002JE001885.
Mangold, N., and P. Allemand (2001), Topographic analysis of features related to ice on Mars, *Geophys. Res. Lett.*, *28*, 407–410.
Maxwell, T. A., and G. E. McGill (1988), Ages of fracturing and resurfacing in the Amenthes region, Mars, *Proc. Lunar Planet. Sci. Conf.*, *18*, 701–711.
McCauley, J. F. (1973), Mariner 9 evidence for wind erosion in the equatorial and midlatitude regions of Mars, *J. Geophys. Res.*, *78*, 4123–4137.
McGill, G. E. (2000), Crustal history of north central Arabia Terra, Mars, *J. Geophys. Res.*, *105*, 6945–6959.
McGill, G. E., and A. M. Dimitriou (1990), Origin of the Martian global dichotomy by crustal thinning in the late Noachian or early Hesperian, *J. Geophys. Res.*, *95*, 12,595–12,605.
McGill, G. E., and S. W. Squyres (1991), Origin of the Martian crustal dichotomy: Evaluating hypotheses, *Icarus*, *93*, 386–393.
Mellon, M. T., B. M. Jakosky, H. H. Kieffer, and P. R. Christensen (2000), High-resolution thermal inertia mapping from the Mars Global Surveyor Thermal Emission Spectrometer, *Icarus*, *148*, 437–455.
Mutch, T. A., R. E. Arvidson, J. W. Head III, K. L. Jones, and R. S. Saunders (1976), *The Geology of Mars*, 400 pp., Princeton Univ., Princeton, N. J.
Neukum, G., and K. Hiller (1981), Martian ages, *J. Geophys. Res.*, *86*, 3097–3121.
Nowicki, S. A., and P. R. Christensen (1999), Mars surface rock abundance from Thermal Emission Spectrometer (TES) mapping data, paper presented at Fifth Int. Mars Conf., Lunar Planet. Inst., Houston, Texas.
Parker, T. J., R. S. Saunders, and D. M. Schneeberger (1989), Transitional morphology in West Deuteronilus Mensae, Mars: Implications for modification of the lowland/upland boundary, *Icarus*, *82*, 111–145.
Parker, T. J., D. S. Gorsline, R. S. Saunders, D. C. Pieri, and D. M. Schneeberger (1993), Coastal geomorphology of the Martian northern plains, *J. Geophys. Res.*, *98*, 11,061–11,078.
Pelkey, S. M., and B. M. Jakosky (2002), Surficial geologic surveys of Gale Crater and Melas Chasma, Mars: Integration of remote-sensing data, *Icarus*, *160*, 228–257.
Pelkey, S. M., B. M. Jakosky, and P. R. Christensen (2004), Surficial properties in Gale Crater, Mars, from Mars Odyssey THEMIS data, *Icarus*, *167*, 244–270.
Presley, M. A., and P. R. Christensen (1997), Thermal conductivity measurements of particulate materials: 2. Results, *J. Geophys. Res.*, *102*, 6551–6566.
Putzig, N. E., M. T. Mellon, and R. E. Arvidson (2003), Thermophysical properties of the Martian south polar region, paper presented at Sixth Int. Mars Conf., Lunar Planet. Inst., Houston, Texas.
Pye, K. (1987), *Aeolian Dust and Dust Deposits*, 334 pp., Academic, San Diego, Calif.
Sakimoto, S. E. H., H. V. Frey, J. B. Garvin, and J. H. Roark (1999), Topography, roughness, layering, and slope properties of the Medusae Fossae Formation from Mars Orbiter Laser Altimeter (MOLA) and Mars Orbiter Camera (MOC) data, *J. Geophys. Res.*, *104*, 24,141–24,154.
Scott, D. H., and J. W. Allingham (1976), Geologic map of the Elysium quadrangle of Mars, *U.S. Geol. Surv. Map, I-935 (MC-15)*.
Scott, D. H., and K. L. Tanaka (1986), Geologic map of the western equatorial region of Mars, *U.S. Geol. Surv. Map, I-1802–A*.
Scott, D. H., E. C. Morris, and M. N. West (1978), Geologic map of the Aeolis quadrangle of Mars, *U.S. Geol. Surv. Map, I-1111 (MC-23)*.
Sharp, R. P. (1973), Mars: Fretted and chaotic terrains, *J. Geophys. Res.*, *78*, 4073–4083.
Sleep, N. H. (1994), Martian plate tectonics, *J. Geophys. Res.*, *99*, 5639–5655.
Smith, D. E., et al. (2001), Mars Orbiter Laser Altimeter: Experiment summary after the first year of global mapping of Mars, *J. Geophys. Res.*, *106*, 23,689–23,722.
Soderblom, L. A., M. C. Malin, J. A. Cutts, and B. C. Murray (1973), Mariner 9 observations of the surface of Mars in the north polar region, *J. Geophys. Res.*, *78*, 4197–4210.
Squyres, S. W. (1978), Martian fretted terrain: Flow of erosional debris, *Icarus*, *34*, 600–613.
Strom, R. G., S. K. Croft, and N. D. Barlow (1992), The martian impact cratering record, in *Mars*, edited by H. H. Kieffer et al., pp. 383–423, Univ. of Ariz. Press, Tucson.
Tanaka, K. L. (1986), The stratigraphy of Mars, *J. Geophys. Res.*, *91*, E139–E158.
Tanaka, K. L., M. G. Chapman, and D. H. Scott (1992), Geologic map of the Elysium region of Mars, *U.S. Geol. Surv. Map, I-2147*.
Tanaka, K. L., J. A. Skinner Jr., T. M. Hare, T. Joyal, and A. Wenker (2003), Resurfacing history of the northern plains of Mars based on geologic mapping of Mars Global Surveyor data, *J. Geophys. Res.*, *108*(E4), 8043, doi:10.1029/2002JE001908.
Taylor, P. A., P. J. Mason, and E. F. Bradley (1987), Boundary-layer flow over low hills (a review), *Boundary Layer Meteorol.*, *39*, 107–132.
Walmsey, J. L., J. R. Salmon, and P. A. Taylor (1982), On the application of a model of boundary-layer flow over low hills to real terrain, *Boundary Layer Meteorol.*, *23*, 17–46.
Ward, A. W. (1979), Yardangs on Mars: Evidence of recent wind erosion, *J. Geophys. Res.*, *84*, 8147–8166.
Watters, T. R. (2003a), Lithospheric flexure and the origin of the dichotomy boundary on Mars, *Geology*, *31*, 271–274.
Watters, T. R. (2003b), Thrust faults along the dichotomy boundary in the eastern hemisphere of Mars, *J. Geophys. Res.*, *108*(E6), 5054, doi:10.1029/2002JE001934.
Watters, T. R., and M. S. Robinson (1999), Lobate scarps and the Martian crustal dichotomy, *J. Geophys. Res.*, *104*, 18,981–18,990.
Wells, G. L., and J. R. Zimbelman (1997), Extraterrestrial arid surface processes, in *Arid Zone Geomorphology: Process, Form, and Change in Drylands*, 2nd ed., edited by D. S. G. Thomas, pp. 659–690, John Wiley, Hoboken, N. J.
Wilhelms, D. E., and S. W. Squyres (1984), The Martian hemispheric dichotomy may be due to a giant impact, *Nature*, *309*, 138–140.
Wise, D. U., M. P. Golombeck, and G. E. McGill (1979), Tharsis province of Mars: Geologic sequence, geometry, and a deformation mechanism, *Icarus*, *38*, 456–472.
Zhong, S., and M. T. Zuber (2001), Degree-1 mantle convection and the crustal dichotomy on Mars, *Earth Planet. Sci. Lett.*, *189*, 75–84.
Zuber, M. T. (2001), The crust and mantle of Mars, *Nature*, *412*, 220–227.
Zurek, R. W., J. R. Barnes, R. M. Haberle, J. B. Pollack, J. E. Tillman, and C. B. Leovy (1992), Dynamics of the atmosphere of Mars, in *Mars*, edited by H. H. Kieffer et al., pp. 835–933, Univ. of Ariz. Press, Tucson.

A. D. Howard, Department of Environmental Sciences, University of Virginia, Charlottesville, VA 22904, USA. (ah6p@virginia.edu)

R. P. Irwin III, T. R. Watters, and J. R. Zimbelman, Center for Earth and Planetary Studies, National Air and Space Museum, Smithsonian Institution, 6th St. and Independence Ave. SW, Washington, DC 20013-7012, USA. (irwinr@nasm.si.edu; watters@nasm.si.edu; jrz@nasm.si.edu)